

Infrared Regularization and Finite Size Dynamics of Entanglement Entropy in Schwarzschild Black Hole

D.S. Ageev^{a,*}, I.Ya. Aref'eva^{a,†}, A.I. Belokon^{a,‡}, A.V. Ermakov^{b,§}, V.V. Pushkarev^{a,¶} and T.A. Rusalev^{a,**}

^a*Steklov Mathematical Institute, Russian Academy of Sciences,
Gubkin str. 8, 119991 Moscow, Russian Federation*

^b*Department of Physics and Astronomy, University of Manchester,
Oxford Road, M13 9PL Manchester, England, United Kingdom*

(Dated: May 24, 2023)

In this paper, infrared regularization of semi-infinite entangling regions and island formation for regions of finite size in the eternal Schwarzschild black hole are considered. We analyze the validity of the complementarity property of entanglement entropy, assumed in previous studies, and elaborate the direct calculation of entanglement entropy for infinite regions. We show that an arbitrary regularization of infinities generally violates complementarity and pure state condition. We introduce the infrared regularization that respects these two properties. Our result is that we derive two fundamental types of finite regions, which we call “mirror-symmetric” (MS) and “asymmetric” (AS). For MS regions, we discover a discontinuous evolution of the entanglement entropy of Hawking radiation due to finite lifetime of the island. The entanglement entropy of matter does not follow the Page curve for semi-infinite regions in two-sided Schwarzschild black hole. For AS regions, the time evolution is bounded from above due to the phenomenon that we call “Cauchy surface breaking”. Shortly before the break, the island configuration gets non-symmetric. For both types, there is a critical size of the region, below which the island never dominates. For regions smaller than some other critical size, the island does not emerge. Finally, we show that the island prescription does not help to solve the information paradox for certain finite size regions.

I. INTRODUCTION

Hawking radiation is a phenomenon which opens up the window into the world of quantum effects emerging in gravity [1, 2]. Years ago, Page showed [3, 4] that a detailed comparison of the thermodynamic entropy of black holes and the entanglement entropy of their radiation results in the observation that the latter exhibits an unlimited growth and finally exceeds the Bekenstein-Hawking entropy. This is in contradiction with the expected time dependence of the entanglement entropy visualized by the Page curve, which should start to decrease after a certain point, called the Page time. The descending part of the Page curve is difficult to interpret in a straightforward way, and recently a new mechanism called the “entanglement islands” was introduced [5–7] to explain the stoppage of the entanglement entropy growth. This mechanism arises for systems with dynamical gravitational degrees of freedom. The conjecture of modifying the entanglement entropy in the presence of dynamical gravity has attracted a lot of attention in recent years [8–76]. The entanglement islands has been studied in the setups of two-dimensional gravity [5, 12, 14, 15, 24, 25, 29, 35, 55], boundary CFT [13, 19, 43, 49, 60, 62–64, 67, 70, 76] and moving mirror models [8–11, 33, 37, 38, 45, 52, 69].

In this paper, we study the properties of entanglement entropy and islands in the four-dimensional Schwarzschild black hole following the s-wave approximation, proposed in [5] and used in the context of higher-dimensional black holes in [18]. This approximation, having been applied to the fields defined on the background of a higher-dimensional Schwarzschild black hole, effectively reduces the problem to a two-dimensional one. The model [18] explains how the entanglement entropy, associated with semi-infinite regions “collecting” Hawking radiation, saturates after taking into account the contribution of the entanglement island in the outer near-horizon zone of two-sided Schwarzschild black hole. The variety of papers exploiting the s-wave approximation in different contexts have been published recently [22, 30, 31, 35, 36, 41, 44, 46, 48, 51, 53, 55, 56, 61, 65, 66, 68, 71–73].

We generalise the results of [18] by considering Hawking quanta as free massless Dirac fermions collected in entangling regions of finite extent. This problem reveals curious features of entanglement entropy in two-sided Schwarzschild black hole. It is well known [77, 78] that the entanglement entropy of a pure state is exactly zero, and if this state is bipartite then the entropies of each partition are equal. In the following, we call these properties “pure state condition” and “complementarity”, respectively. The latter is commonly used in the calculations of the entanglement entropy for semi-infinite regions [18, 22, 28, 41, 74].

In Section III, we explicitly check whether these two properties hold, i.e.

$$S(\text{pure state}) \stackrel{?}{=} 0, \quad (1)$$

$$S(R) \stackrel{?}{=} S(\overline{R}), \quad (2)$$

* ageev@mi-ras.ru

† arefeva@mi-ras.ru

‡ belokon@mi-ras.ru

§ alexey.ermakov@manchester.ac.uk

¶ pushkarev@mi-ras.ru

** rusalev@mi-ras.ru

and unveil, strictly speaking, that they are *violated*. We consider the simplest configurations of entangling regions and derive the regularization prescription that allows complementarity and pure state condition to be satisfied in two-sided Schwarzschild black hole.

In Section IV, we study the time evolution of the entanglement entropy of Hawking radiation for two fundamental types of finite entangling regions, including their island phase.

In Section V, we discuss the information paradox in the context of finite entangling regions.

A brief overview of the setup is given in Section II. Section VI contains a short summary and future perspectives. Some technical details have been moved to Appendix A for the purpose of readability.

II. SETUP

A. Geometry

We start with the metric of the four-dimensional Schwarzschild black hole

$$ds^2 = -f(r)dt^2 + \frac{dr^2}{f(r)} + r^2 d\Omega_2^2, \quad f(r) = 1 - \frac{r_h}{r}, \quad (3)$$

where r_h denotes the black hole horizon, and $d\Omega_2^2$ is the angular part of the metric. Introducing Kruskal coordinates, which for the right wedge take the form

$$U = -\frac{1}{\kappa_h} e^{-\kappa_h(t-r_*(r))}, \quad V = \frac{1}{\kappa_h} e^{\kappa_h(t+r_*(r))}, \quad (4)$$

with the tortoise coordinate $r_*(r) = r + r_h \ln[(r - r_h)/r_h]$ and the surface gravity $\kappa_h = 1/2r_h$, we can rewrite the metric in the form

$$ds^2 = -e^{2\rho(r)} dU dV + r^2 d\Omega_2^2, \quad (5)$$

with the conformal factor $e^{2\rho(r)}$ given by

$$e^{2\rho(r)} = \frac{e^{-2\kappa_h r}}{2\kappa_h r}. \quad (6)$$

In what follows, we need a formula for the radial distance $d(\mathbf{x}, \mathbf{y})$ for the spherically symmetric two-dimensional part of the metric. If we consider (5) as a Weyl transformed version of the metric $ds^2 = -dU dV$ (neglecting the angular part) with the Weyl factor $e^{2\rho(r)}$, the square of the distance $d(\mathbf{x}, \mathbf{y})$ can be derived as

$$d^2(\mathbf{x}, \mathbf{y}) = e^{\rho(\mathbf{x})} e^{\rho(\mathbf{y})} [U(\mathbf{x}) - U(\mathbf{y})] [V(\mathbf{y}) - V(\mathbf{x})], \quad (7)$$

where bold letters denote pairs of radial and time coordinates, e.g., $\mathbf{x} = (x, t_x)$. In terms of (t, r) -coordinates, the distance reads

$$d^2(\mathbf{x}, \mathbf{y}) = \frac{2\sqrt{f(x)f(y)}}{\kappa_h^2} \times [\cosh \kappa_h(r_*(x) - r_*(y)) - \cosh \kappa_h(t_x - t_y)]. \quad (8)$$

We use the following notation for spacetime points in the right and left wedges of the Penrose diagram, respectively

$$\mathbf{x}_+ = (x_+, t_{x_+}), \quad \mathbf{x}_- = \left(x_-, t_{x_-} + \frac{i\pi}{\kappa_h}\right).$$

Note that the imaginary part of the time coordinate implies that \mathbf{x}_- is in the left wedge.

By the *infrared limit* of the point \mathbf{x} , we mean that \mathbf{x} tends to spacelike infinity i^0 in the corresponding wedge along an arbitrary spacelike curve: $t_x = t_x(x)$.

B. Entanglement entropy

We study the entanglement entropy of conformal matter represented by free Dirac fermions on the background (3). Generally speaking, the calculation of entanglement entropy in a higher-dimensional curved spacetime is an extremely challenging problem. An important suggestion made in [18] is to consider the s-wave approximation. The fact that a static observer at spatial infinity collects predominantly lower multipoles, while the higher ones backscatter in the Schwarzschild black hole potential, reduces the initially complicated setup to a simpler two-dimensional problem of calculation the entanglement entropy of conformal matter.

The entanglement entropy of c free massless Dirac fermions for a system of N intervals [79] in the curved background (3) reads

$$S_m = \frac{c}{3} \sum_{i,j} \ln \frac{d(\mathbf{x}_i, \mathbf{y}_j)}{\varepsilon} - \frac{c}{3} \sum_{i < j} \ln \frac{d(\mathbf{x}_i, \mathbf{x}_j)}{\varepsilon} - \frac{c}{3} \sum_{i < j} \ln \frac{d(\mathbf{y}_i, \mathbf{y}_j)}{\varepsilon}, \quad (9)$$

where the distance $d(\mathbf{x}_i, \mathbf{y}_j)$ is given by (8), \mathbf{x}_i and \mathbf{y}_i denote the left and right endpoints of the corresponding intervals, and ε is a UV cutoff.

C. Generalized entropy functional

Recently, it was proposed [5, 7, 15, 80] that the expected behavior of the Page curve emerges from the island prescription. Considering the Hartle-Hawking vacuum [81], the reduced density matrix of Hawking radiation collected in R is defined by tracing out the states in the complement region \bar{R} , which includes the black hole interior. The island mechanism prescribes that the states in some regions $I \subset \bar{R}$, called entanglement islands, are to be excluded from tracing out.

The island contribution can be taken into account via the generalized entropy functional defined as [14, 15]

$$S_{\text{gen}}[I, R] = \frac{\text{Area}(\partial I)}{4G_N} + S_m(R \cup I). \quad (10)$$

Here ∂I denotes the boundary of the entanglement island, G_N is Newton's constant, and S_m is the entanglement entropy of conformal matter. One should extremize this functional over all possible island configurations

$$S_{\text{gen}}^{\text{ext}}[I, R] = \text{ext}_{\partial I} \left\{ S_{\text{gen}}[I, R] \right\}, \quad (11)$$

and then choose the minimal one

$$S(R) = \min_{\partial I} \left\{ S_{\text{gen}}^{\text{ext}}[I, R] \right\}. \quad (12)$$

III. INFRARED REGULARIZATION AND COMPLEMENTARITY PROPERTY

In this section, we consider different partitions of Cauchy surfaces and derive regularization rules for space-like infinities in order to be consistent with fundamental properties of entanglement entropy.

The importance of a proper regularization can be seen from the following illustration. Previous papers (see for example [18, 22, 28, 41, 74]) have used extensively the calculation of the entropy for finite complements of entangling regions. In particular, the entanglement entropy for the semi-infinite region $R_\infty \equiv R_- \cup R_+ = (i^0, \mathbf{b}_-) \cup [\mathbf{b}_+, i^0)$, where the Hawking radiation is collected, is actually calculated in [18] using the complementarity property

$$S_m(R_\infty) = S_m(\bar{R}_\infty), \quad (13)$$

with the complement $\bar{R}_\infty = [\mathbf{b}_-, \mathbf{b}_+]$ (see Fig. 1). The calculation of $S_m(\bar{R}_\infty)$ leads to [18]

$$S_m(\bar{R}_\infty) = \frac{c}{6} \ln \left(\frac{4f(b)}{\kappa_h^2 \varepsilon^2} \cosh^2 \kappa_h t_b \right). \quad (14)$$

In the limit when the boundaries of the entangling regions are sent to spacelike infinities i^0 along the same timeslices (i.e., $b \rightarrow \infty$ at fixed t_b), this formula reduces to

$$\lim_{b \rightarrow \infty} S_m(\bar{R}_\infty) = \frac{c}{3} \ln \frac{2}{\kappa_h \varepsilon} + \frac{c}{3} \ln \cosh \kappa_h t_b. \quad (15)$$

This is not what to be expected, since in this limit of the vanishingly small region R_∞ , entangled particles of radiation are not collected, and the entanglement entropy (14) should have been equal to zero. However, the result grows linearly at late times. This raises the question on the structure of semi-infinite entangling regions from the geometrical point of view.

A. Warm-up: complementarity and pure state condition in CFT in flat background

Before considering the curved geometry of two-sided Schwarzschild black hole, we recall the subtleties related

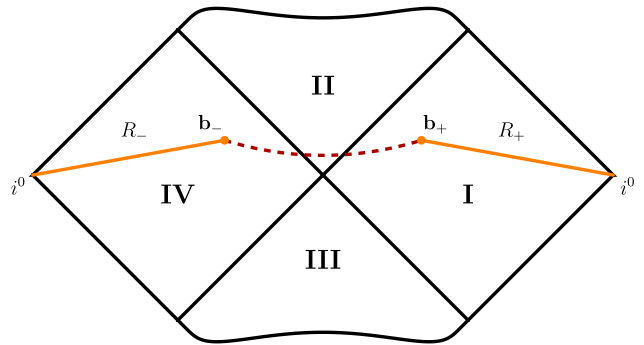


Figure 1. Penrose diagram for the eternal Schwarzschild black hole with the *schematic* plots of the entangling region $R_\infty \equiv R_- \cup R_+$ (orange) and its complement $\bar{R}_\infty \equiv [\mathbf{b}_-, \mathbf{b}_+]$ (dashed dark red).

to the calculation of the entanglement entropy for an infinite region in flat two-dimensional CFT.

Let us consider an interval $R = [-\ell/2, \ell/2]$ on the plane \mathbb{R}^2 with coordinates (x, τ) at a constant time $\tau = 0$. It is well known [82, 83] that the entanglement entropy for this subsystem is

$$S_m(R) = \frac{c}{3} \ln \frac{\ell}{\varepsilon} + c'_1, \quad (16)$$

where c'_1 is some model-dependent constant, which is known only for several integrable systems. The complement of this interval is the region

$$\bar{R} = \left(-\infty, -\frac{\ell}{2} \right] \cup \left[\frac{\ell}{2}, +\infty \right).$$

There are two qualitatively different approaches to calculate the entanglement entropy for a semi-infinite region such as \bar{R} :

- to consider the entangling region $[-\ell/2, \ell/2]$ with its regularized complement $[-L/2, -\ell/2] \cup [\ell/2, L/2]$, and then take the limit $L \rightarrow \infty$ to obtain semi-infinite regions (without changing the geometry, see Fig. 2);
- for the entangling region $[-\ell/2, \ell/2]$ cut the underlying geometry by introducing a system with the boundaries at $\pm L/2$, and then take the limit of infinite geometry $L \rightarrow \infty$ (see Fig. 3 for the case with periodic boundary conditions).

In both cases, L might be seen as an infrared cutoff.

Following the first approach, let us calculate the entanglement entropy of the regularized complement

$$\bar{R}_{\text{reg}} = \left[-\frac{L}{2}, -\frac{\ell}{2} \right] \cup \left[\frac{\ell}{2}, \frac{L}{2} \right]$$

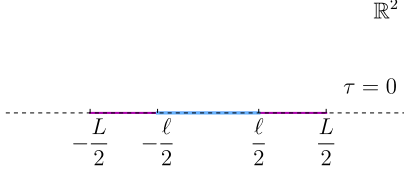


Figure 2. Regularized region $[-L/2, L/2]$ with the interval $[-\ell/2, \ell/2]$ (blue) and its complement (magenta) on the line $\tau = 0$ in \mathbb{R}^2 .

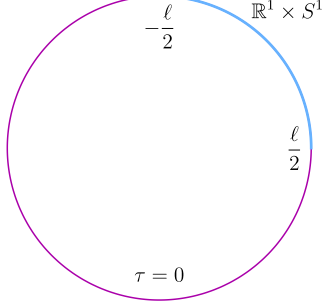


Figure 3. The interval $[-\ell/2, \ell/2]$ (blue) and its complement (magenta) on the line $\tau = 0$ of the cylinder $\mathbb{R}^1 \times S^1$ with circumference L .

on the whole line $\tau = 0$ (see Fig. 2)

$$S_m(\overline{R}_{\text{reg}}) = \frac{c}{3} \ln \left(\frac{\ell L(L - \ell)^2}{\varepsilon^2(L + \ell)^2} \right). \quad (17)$$

This expression diverges as $\ln L$ at $L \rightarrow \infty$. Even though we consider a pure state, we get that the complementarity property $S_m(R) = S_m(\overline{R})$ between the entropies for a finite interval and its infinite complement is formally violated. Moreover, for a pure state, the entropy of the whole system should be equal to zero: $S_m(R \cup \overline{R}) = 0$, while the entropy for the interval (16) also diverges logarithmically at $\ell \rightarrow \infty$.

In the second approach, the physical properties of an infinite system can be obtained from its formulation in a finite-size geometry by imposing various boundary conditions. The entropy for an interval of length ℓ on a cylinder (periodic boundary conditions), whose circumference L plays the role of the infrared cutoff (see Fig. 3), is given by

$$S_m(R) = \frac{c}{3} \ln \left(\frac{L}{\pi \varepsilon} \sin \frac{\pi \ell}{L} \right) + c'_1. \quad (18)$$

Due to the symmetry $\ell \leftrightarrow L - \ell$ of this expression, the complementarity holds automatically. When the whole system is considered, i.e., $\ell = L$ (in fact, $\ell = L - \varepsilon$ for the system on a lattice), the entanglement entropy (18) is zero up to a non-universal constant c'_1 . In the limit

$L \rightarrow \infty$, the entanglement entropy (16) for an interval on a plane \mathbb{R}^2 is reproduced.

Note that the entanglement entropy in a curved geometry can be obtained from that in flat space by the Weyl transformation, which leads to conformal factors in the distance (7). For the Schwarzschild geometry, the conformal factor is given by (6) and tends to zero at $r \rightarrow \infty$. Due to this fact, one can get a finite distance between spacelike infinities in the left and right wedges without imposing periodic or open boundary conditions.

B. Infrared regularization of Cauchy surfaces

Let us introduce the infrared regularization of a Cauchy surface Σ which extends between spacelike infinities in the left and right wedges (see Fig. 4). Since the Hartle–Hawking state given on Σ is pure, we *expect* that for the entanglement entropy we get: $S_m(\Sigma) = 0$. To regularize Σ , we take a finite spacelike interval $\Sigma_{\text{reg}} \subset \Sigma$ such that $\Sigma_{\text{reg}} = [\mathbf{q}_-, \mathbf{q}_+]$ with the following coordinates of the IR regulators \mathbf{q}_{\pm}

$$\mathbf{q}_+ = (q_+, t_{q_+}(q_+)), \quad \mathbf{q}_- = \left(q_-, t_{q_-}(q_-) + \frac{i\pi}{\kappa_h} \right).$$

Then, the entanglement entropy of conformal matter on the regularized Cauchy surface Σ_{reg} is given by

$$\begin{aligned} S_m(\Sigma_{\text{reg}}) &= \frac{c}{3} \ln \frac{d(\mathbf{q}_-, \mathbf{q}_+)}{\varepsilon} = \\ &= \frac{c}{6} \ln \left[\frac{2\sqrt{f(q_+)f(q_-)}}{\kappa_h^2 \varepsilon^2} \left(\cosh \kappa_h(r_*(q_+) - r_*(q_-)) + \right. \right. \\ &\quad \left. \left. + \cosh \kappa_h(t_{q_+}(q_+) - t_{q_-}(q_-)) \right) \right], \end{aligned} \quad (19)$$

which is, in general, divergent in the IR limit $q_{\pm} \rightarrow \infty$. However, this limit exists along the curves \mathcal{C} of the following type

$$\mathcal{C}: \quad \begin{aligned} \kappa_h(r_*(q_+) - r_*(q_-)) &= c_1 + \alpha(q_+, q_-), \\ \kappa_h(t_{q_+}(q_+) - t_{q_-}(q_-)) &= c_2 + \beta(q_+, q_-), \end{aligned} \quad (20)$$

where c_1 and c_2 are arbitrary constants fixed for a particular curve, and

$$\lim_{q_{\pm} \rightarrow \infty} \alpha(q_+, q_-) = 0, \quad \lim_{q_{\pm} \rightarrow \infty} \beta(q_+, q_-) = 0.$$

Taking into account that $f(q_{\pm}) \rightarrow 1$ as $q_{\pm} \rightarrow \infty$, the IR limit of (19) along some curve \mathcal{C} (20) is given by

$$S_m(\Sigma) = \lim_{\substack{q_{\pm} \rightarrow \infty \\ \mathbf{q}_{\pm} \in \mathcal{C}}} S_m(\Sigma_{\text{reg}}) = \frac{c}{3} \ln \frac{2}{\kappa_h \varepsilon} + F(c_1, c_2), \quad (21)$$

where

$$F(c_1, c_2) \equiv \frac{c}{6} \ln \left(\frac{\cosh c_1 + \cosh c_2}{2} \right) \geq 0. \quad (22)$$

Since this function is non-negative, the entanglement entropy can take any positive value by varying the constants c_1, c_2 . For the same reason, we cannot get rid of the first term on the RHS of (21) by an appropriate choice of the constants c_1, c_2 . The best we can get is to let $c_1 = c_2 = 0$, which according to (20) leads to

$$\lim_{\substack{q_{\pm} \rightarrow \infty \\ q_{\pm} \in \mathcal{C}}} (q_+ - q_-) = 0, \quad \lim_{\substack{q_{\pm} \rightarrow \infty \\ q_{\pm} \in \mathcal{C}}} (t_{q_+}(q_+) - t_{q_-}(q_-)) = 0.$$

This means that the IR limit is taken to be asymptotically radially symmetric, and the regulators, as they go to spacelike infinity, asymptotically approach the same timeslice. For this case, the entropy of the Hartle-Hawking state defined on Σ is given by

$$S_m(\Sigma) \Big|_{c_1=c_2=0} = \frac{c}{3} \ln \frac{2}{\kappa_h \varepsilon}. \quad (23)$$

Since the entropy of a pure state should be zero, we claim that this anomalous term is to be subtracted from final answers.

At first sight, it might seem surprising that the result in the IR limit (23) depends on the UV cutoff ε . In fact, this is to be expected, since ε is the only dimensional constant, in addition to r_h , to make the whole answer dimensionless.

The reasons why we get the entanglement entropy for infinite intervals that is not infrared divergent are the special behavior of the Weyl factor (6) at infinity, and the mutual asymptotic cancellation of the regulators. The presence of two regulators of the same sign, which cancel each other in final results, is the hallmark of two-sidedness and higher dimensionality¹ of the eternal Schwarzschild black hole geometry, and cannot be seen as a general method of regularization of infinities during the calculation of entanglement entropy for infinite regions.

C. Infrared regularization of semi-infinite complement of finite entangling regions

A Cauchy surface can be divided into any number of finite entangling regions. A single finite region can lie entirely in one wedge or be extended over two. Regardless, the complement \bar{R} includes two semi-infinite intervals in each wedge, which stretch to the corresponding spacelike

¹ In fact, there are two different static patches (t, r) in two-sided Schwarzschild — in the left and right wedges, respectively. Spacelike infinities $r \rightarrow \infty$ are positive due to the positiveness of the radial coordinate $r \geq 0$, which can be introduced for space-times of higher dimensionality. For example, this is not applicable for two-dimensional Minkowski spacetime, in which spatial coordinate $x \in (-\infty, \infty)$. Therefore, there are two spacelike infinities of different signs: $x \rightarrow \pm\infty$. This leads to the IR divergent entanglement entropy for the Cauchy surface: $S \propto \ln L$ as $L \rightarrow \infty$.

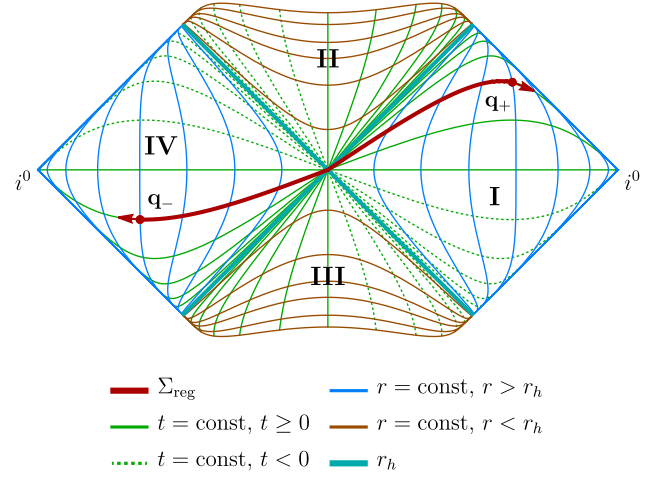


Figure 4. Penrose diagram for the eternal Schwarzschild black hole with the regularized Cauchy surface $\Sigma_{\text{reg}} \equiv [q_-, q_+]$. Arrows highlight that the regulators tend to spacelike infinities, $q_{\pm} \rightarrow i^0$.

infinities i^0 . Our goal is to represent the complement as the IR limit of some finite regions (see Fig. 5). One can consider this procedure as a regularization of spacelike infinities. In this way, the endpoints are defined as

$$\mathbf{y}_+ = (y, t_y), \quad \mathbf{b}_+ = (b, t_b), \quad \mathbf{b}_- = \left(b, t_b + \frac{i\pi}{\kappa_h}\right),$$

$$\mathbf{q}_+ = \left(q_+, t_{q_+}(q_+)\right), \quad \mathbf{q}_- = \left(q_-, t_{q_-}(q_-) + \frac{i\pi}{\kappa_h}\right).$$

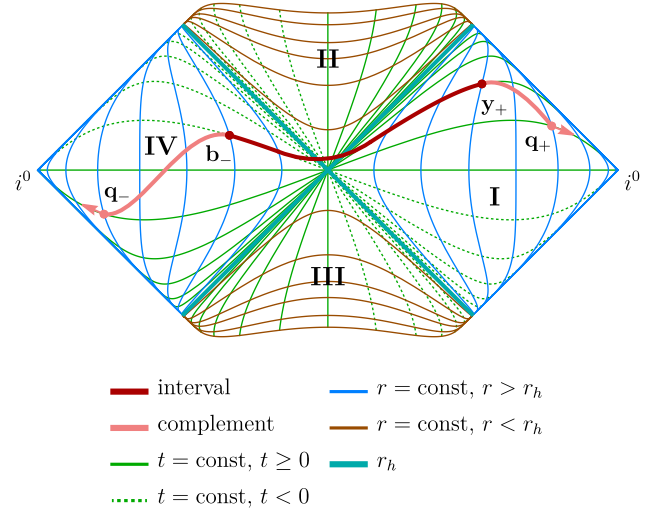


Figure 5. Penrose diagram for the eternal Schwarzschild black hole with the regularized finite interval configuration: the finite interval $[b_-, y_+]$ (dark red) and its regularized complement $[q_-, b_-] \cup [y_+, q_+]$ (light red). Arrows mean that the regulators tend to spacelike infinities, $q_{\pm} \rightarrow i^0$.

Now we want to check the complementarity property $S(R) = S(\bar{R})$ for the region R and its complement \bar{R} . In gravitational theories, both $S(R)$ and $S(\bar{R})$ are determined by the island formula (12), which contains the “area term” and the matter contribution S_m . If the island I is the same both for R and \bar{R} , to verify $S(R) = S(\bar{R})$, it suffices to compare the entanglement entropies of matter only, $S_m(R \cup I) = S_m(\bar{R} \cup I)$. Indeed, in this case, the island formulas for the region R and the complement \bar{R} yield the same, because the same expression is extremized in (12). Therefore, further in this section, we consider only the entanglement entropy of matter S_m .

The entanglement entropy for the region $R = [\mathbf{b}_\pm, \mathbf{y}_+]$ reads

$$S_m(R) = \frac{c}{3} \ln \frac{d(\mathbf{b}_\pm, \mathbf{y}_+)}{\varepsilon}. \quad (24)$$

We compare this with the entanglement entropy for the regularized complement $\bar{R}_{\text{reg}} = [\mathbf{q}_-, \mathbf{b}_\pm] \cup [\mathbf{y}_+, \mathbf{q}_+]$

$$S_m(\bar{R}_{\text{reg}}) = \frac{c}{3} \ln \frac{d(\mathbf{b}_\pm, \mathbf{y}_+)}{\varepsilon} + \frac{c}{3} \ln \frac{d(\mathbf{q}_-, \mathbf{q}_+)}{\varepsilon} + \frac{c}{3} \ln \left[\frac{d(\mathbf{y}_+, \mathbf{q}_+)d(\mathbf{b}_\pm, \mathbf{q}_-)}{d(\mathbf{y}_+, \mathbf{q}_-)d(\mathbf{b}_\pm, \mathbf{q}_+)} \right]. \quad (25)$$

The third term on the RHS tends to zero in the IR limit taken along any spacelike curve. This is because the distance to the regulator \mathbf{q}_+ in the numerator has a counterpart in the denominator, and both have similar asymptotic behavior. The same holds for the distances to the regulator \mathbf{q}_- . Due to the generically divergent distance between the regulators encountered in the second term on the RHS, the IR limit of this expression exists only along the curves given by \mathcal{C} (20) and yields

$$\lim_{\substack{q_\pm \rightarrow \infty \\ \mathbf{q}_\pm \in \mathcal{C}}} S_m(\bar{R}_{\text{reg}}) = S_m(R) + \frac{c}{3} \ln \frac{2}{\kappa_h \varepsilon} + F(c_1, c_2), \quad (26)$$

This result does *not* depend on the wedge (left, right or both) in which the finite entangling region is located. The last two terms of this expression are exactly the same as we get when regularizing a Cauchy surface (21).

It is straightforward to extend this calculation to the case when R consists of N disjoint intervals: $R = [\mathbf{a}_1, \mathbf{a}_2] \cup \dots \cup [\mathbf{a}_{2N-1}, \mathbf{a}_{2N}]$. In this case, the entanglement entropy for the regularized complement is given by

$$S_m(\bar{R}_{\text{reg}}) = S_m(R) + \frac{c}{3} \ln \frac{d(\mathbf{q}_-, \mathbf{q}_+)}{\varepsilon} + \frac{c}{3} \ln \left[\frac{d(\mathbf{a}_1, \mathbf{q}_-) \dots d(\mathbf{a}_{2N}, \mathbf{q}_+)}{d(\mathbf{a}_1, \mathbf{q}_+) \dots d(\mathbf{a}_{2N}, \mathbf{q}_-)} \right]. \quad (27)$$

The third term on the RHS, which makes the only difference with the case of a single interval, is vanishingly small in the IR limit along spacelike curves. Along the curves \mathcal{C} (20), the whole expression becomes the same as (26).

D. Infrared regularization consistent with complementarity and pure state condition

Let us sum up the results. We have established that complementarity and pure state condition are violated by the anomalous term (23) and by the function $F(c_1, c_2)$ (22), which depends on arbitrary parameters c_1 and c_2 .

The IR limit of the entropy is well-defined along the special class of curves \mathcal{C} (20) and for any choice of the constants c_1 and c_2 . Since $F(c_1, c_2) \geq 0$, we let $c_1 = c_2 = 0$, for which $F(0, 0) = 0$, to get rid from this contribution. This means that the regulators are to be sent to infinity asymptotically radially symmetric, and as they approach i^0 , they asymptotically fall on the same timeslice.

Then we *prescribe* that we should subtract the anomalous term (23). In the end, we get the entanglement entropy for semi-infinite regions consistent with complementarity and pure state condition. We call this procedure *the infrared regularization*.

Also, let us clarify about the problem we raised at the beginning of this Section, see (15). As we pointed out, the IR limit is to be taken along the curves \mathcal{C} (20), which implies the dependence of the time coordinates of the IR regulators on the radial ones. From this perspective, the interpretation of the limit $b \rightarrow \infty$, that was given for (15), is incorrect, since it was not assumed that the points \mathbf{b}_\pm become the IR regulators.

IV. ENTROPY DYNAMICS FOR FINITE ENTANGLING REGIONS

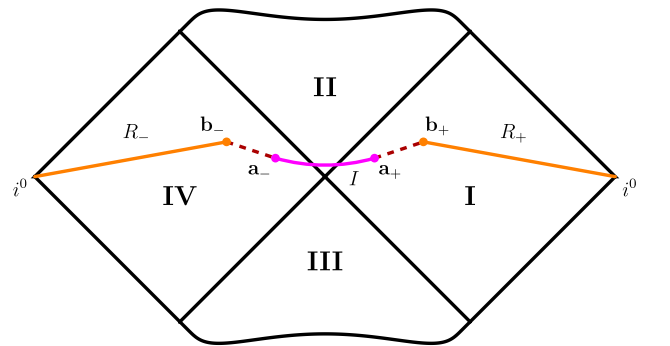


Figure 6. Penrose diagram for the eternal Schwarzschild black hole with the *schematic* plots of semi-infinite entangling region $R_\infty \equiv R_- \cup R_+$ (orange), the entanglement island $I \equiv [\mathbf{a}_-, \mathbf{a}_+]$ (magenta) and their complement $R_- \cup R_+ \cup \bar{I} \equiv [\mathbf{b}_-, \mathbf{a}_-] \cup [\mathbf{a}_+, \mathbf{b}_+]$ (dashed dark red).

In this section, we study the dynamics of finite entangling regions affected by the presence of entangle-

ment islands.

In the original setup [18], which describes semi-infinite entangling region $R_\infty = (i^0, \mathbf{b}_-] \cup [\mathbf{b}_+ i^0)$, the entanglement entropy (14) enters an unbounded linear growth regime at late times $t_b \gg r_h$

$$S_m(R_\infty) \simeq \frac{c}{3} \kappa_h t_b. \quad (28)$$

This can be interpreted as a version of the information paradox. It was shown there that taking into account the contribution of the entanglement island leads to saturation of the entanglement entropy $S(R_\infty)$. At late times, the island is symmetric and its endpoints are located in different wedges near the black hole horizon (see Fig. 6). The entanglement entropy in the leading-order expansion in cG_N/r_h^2 reads

$$S(R_\infty) \Big|_{\text{late times}} \simeq \frac{2\pi r_h^2}{G_N} + \frac{c}{6} \ln \frac{f(b)}{\kappa_h^4 \varepsilon^4} + \frac{c}{6} (2\kappa_h r_*(b) - 1), \quad (29)$$

which is constant in time. We emphasize that this result of [18] fully relies on the complementarity property.

A. Geometry and dynamics of Cauchy surfaces

Up-down notation

We introduce two indices for spacetime points, “up” and “down”, meaning their location with respect to the horizontal line $t = 0$, which stretches between spacelike infinities in the left and right wedges. This notation will prove convenient below. In the following, we use the points

$$\begin{aligned} \mathbf{b}_+^{\text{up}} &= (b, t_b), & \mathbf{b}_-^{\text{up}} &= \left(b, -t_b + \frac{i\pi}{\kappa_h}\right), \\ \mathbf{q}_+^{\text{up}} &= (q, t_b), & \mathbf{q}_-^{\text{up/down}} &= \left(q, \mp t_b + \frac{i\pi}{\kappa_h}\right). \end{aligned} \quad (30)$$

Note that points \mathbf{b}_+ and \mathbf{b}_- have the same radial coordinates. Real parts of their time coordinates are opposite in sign, such a choice makes the problem time-dependent [12, 18]. Also, without loss of generality, we take $\mathbf{q}_\pm^{\text{up/down}}$ radially symmetric.

Dynamics of Cauchy surfaces

Given $N > 2$ points on the Penrose diagram, we can stretch a hypersurface to all of them as well as to the corresponding spacelike infinities i^0 . Here we develop a recipe for how to select these points so that the resulting hypersurface is a Cauchy one.

Let us divide all the points of the regularized Cauchy surface into the inner ones, whose radial coordinates are

fixed and finite, and IR regulators \mathbf{q}_\pm . The latter are the endpoints of the regularized finite hypersurface, which are to be sent to i^0 .

In the following, we discuss the evolution of finite regions of the type $R = [\mathbf{q}_-^{\text{up/down}}, \mathbf{b}_-^{\text{up}}] \cup [\mathbf{b}_+^{\text{up}}, \mathbf{q}_+^{\text{up}}]$ (the intermediate points \mathbf{q}_+^{up} and $\mathbf{q}_-^{\text{up/down}}$, whose radial coordinates are fixed, should not be confused with the IR regulators \mathbf{q}_\pm). Such a choice of the region endpoints is motivated by the following reason. Moving the intermediate points along their Killing vectors ∂_t^+ in the right wedge and ∂_t^- in the left is an isometry of the Schwarzschild spacetime. Thus, we would not get any non-trivial dynamics out of their flow. On the contrary, if we explicitly impose the relations (30), we would get the points in the right wedge moving along their Killing vectors, while in the left edge, those points with $t < 0$ would move upwards to $t \rightarrow -\infty$, and with $t > 0$ — downwards to $t \rightarrow +\infty$. This choice is *not* a symmetry of the problem, therefore, it would generate a non-trivial dynamics of the entropy. [12, 84]

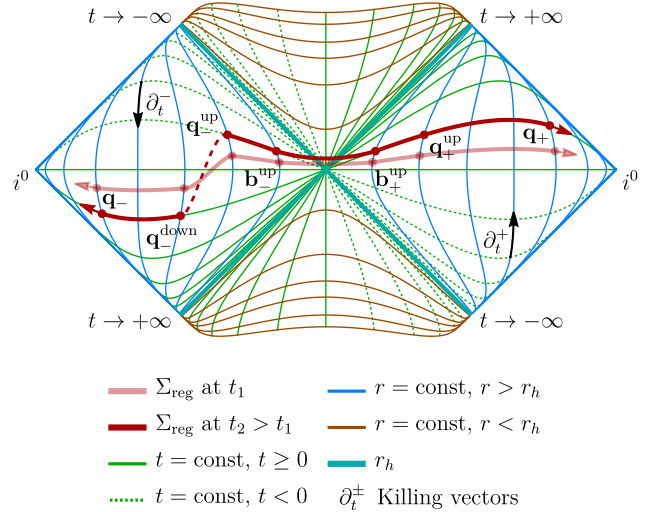


Figure 7. Penrose diagram for the eternal Schwarzschild black hole with a regularized Cauchy surface. During time evolution (from the light red curve to the dark red one) two adjacent intermediate points in the left wedge become timelike separated which breaks the Cauchy surface (dashes).

Having said this, we should emphasize that in the context of finite size regions, the choice of the points (30) has a non-trivial consequence which we call the “Cauchy surface breaking”. This phenomenon takes place when some points get separated during time evolution by a timelike interval (see Fig. 7) due to different directions of their movement on the diagram. When the Cauchy surface breaks, the problem of studying the evolution of entanglement entropy becomes ill-defined, so we should keep track of this phenomenon.

Thus, the recipe of picking a Cauchy surface is as follows:

- a) Since a Cauchy surface is a spacelike hypersurface, all its tangents should be spacelike. For our setup this means that if some of the inner points of a hypersurface in the left wedge lie on different sides with respect to the line $t = 0$, they will eventually become timelike separated. We should either avoid such hypersurfaces or consider their dynamics only for a finite time until the Cauchy surface breaks.
- b) Regulators \mathbf{q}_{\pm} are chosen according to the IR regularization described in Section III D.

Regarding the finite regions R , the Cauchy surface breaking implies:

- c) If the outermost inner point in the left wedge is $\mathbf{q}_{-}^{\text{up}}$, then the sign of its time coordinate is opposite to that of the IR regulator \mathbf{q}_{-} . This fact can naively cause the Cauchy surface breaking. However, by sending the regulator to i^0 , we effectively make the Cauchy surface breaking time infinite.
- d) If the outermost inner point in the left wedge is $\mathbf{q}_{-}^{\text{down}}$, then inevitably the corresponding Cauchy surface breaks, since the distance squared between $\mathbf{q}_{-}^{\text{down}}$ and $\mathbf{b}_{-}^{\text{up}}$ gets negative at some point (see Section IV C).

If the conditions a) – c) are met, then we get a Cauchy surface, on which complementarity and pure state condition are respected. If, instead of c), the option d) takes place, we obtain a hypersurface which gets timelike at some time moment and therefore, the entanglement entropy of Hawking radiation is well-defined only for a finite time.

B. Mirror-symmetric finite entangling region

Let us consider the union of two finite intervals located in the right and left wedges, whose outer boundaries are mirror-symmetric² (see Fig. 8)

$$R_{\text{MS}} \equiv [\mathbf{q}_{-}^{\text{up}}, \mathbf{b}_{-}^{\text{up}}] \cup [\mathbf{b}_{+}^{\text{up}}, \mathbf{q}_{+}^{\text{up}}].$$

We call such a configuration the *mirror-symmetric (MS) finite entangling region*.

The region R_{MS} has a straightforward interpretation. With respect to a static observer, one can imagine each part of R_{MS} as a domain between two concentric spheres with radii b and $q > b$. Outgoing Hawking modes pass through this domain in a finite time and then escape to infinity.

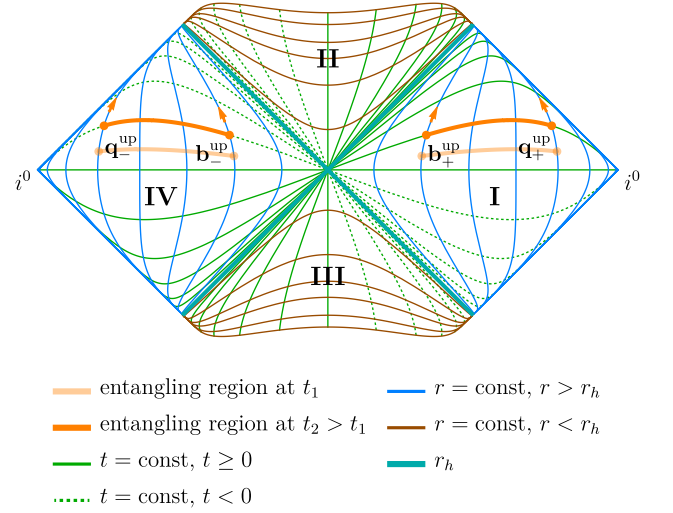


Figure 8. Penrose diagram for the eternal Schwarzschild black hole with a mirror-symmetric entangling region $R_{\text{MS}} \equiv [\mathbf{q}_{-}^{\text{up}}, \mathbf{b}_{-}^{\text{up}}] \cup [\mathbf{b}_{+}^{\text{up}}, \mathbf{q}_{+}^{\text{up}}]$. Arrows indicate the direction of flow of points during time evolution.

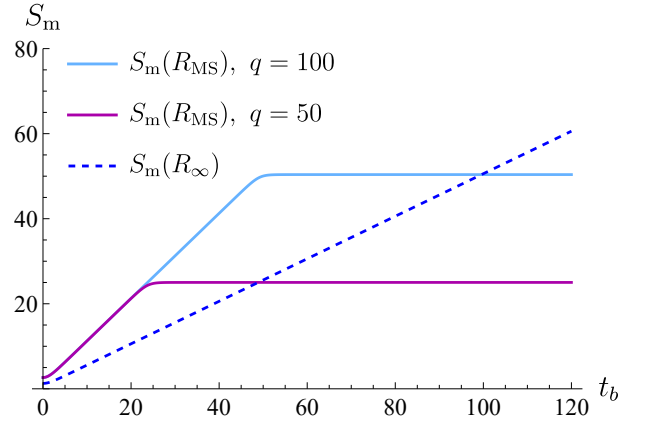


Figure 9. Entropy evolution of MS finite region R_{MS} with $q = 50$ (dark magenta), $q = 100$ (sky blue), and of the semi-infinite region R_{∞} (blue dashed). For all cases, we take $b = 5$, $r_h = 1$, $c = 3$, $\varepsilon = 1$. The monotonic growth of $S_m(R_{\text{MS}})$ is twice as fast compared to $S_m(R_{\infty})$.

The entanglement entropy of Hawking radiation collected in the MS region is given by (see Appendix (A1))

$$S_m(R_{\text{MS}}) = \frac{c}{6} \ln \left(\frac{16f(b)f(q)}{\kappa_h^4 \varepsilon^4} \right) + \frac{c}{3} \ln \cosh^2 \kappa_h t_b + \frac{c}{3} \ln \left(\frac{\cosh \kappa_h (r_*(q) - r_*(b)) - 1}{\cosh \kappa_h (r_*(q) - r_*(b)) + \cosh 2\kappa_h t_b} \right). \quad (31)$$

If the region is large enough, i.e., $q \gg b$, then at intermediate times

$$1 \ll \cosh 2\kappa_h t_b \ll \cosh \kappa_h (r_*(q) - r_*(b)),$$

the entanglement entropy of the radiation increases

² By mirror symmetry we mean the reflection about the vertical axis of symmetry of the Penrose diagram.

monotonically as

$$S_m(R_{\text{MS}}) \Big|_{\text{inter. times}} \simeq \frac{2c}{3} \kappa_h t_b, \quad (32)$$

which is twice as fast as for the semi-infinite region (28). This behavior arises due to the fact that the distance between the points \mathbf{q}_- and \mathbf{q}_+ is now time-dependent, since they lie on different timeslices. Also, provided that $t_b = t_q$, this time dependence is exactly the same as that of the distance between \mathbf{b}_- and \mathbf{b}_+ , which doubles the coefficient.

At late times

$$\cosh 2\kappa_h t_b \gg \cosh \kappa_h (r_*(q) - r_*(b)),$$

the entropy saturates at the value (see Appendix (A3))

$$S_m(R_{\text{MS}}) \Big|_{\text{late times}} \simeq \frac{c}{6} \ln \left(\frac{16f(b)f(q)}{\kappa_h^4 \varepsilon^4} \right) + \frac{c}{3} \ln \left[\cosh \kappa_h (r_*(q) - r_*(b)) - 1 \right]. \quad (33)$$

This can be interpreted as follows. As soon as the “first”³ particle of the black hole radiation reaches $r = b$, the entropy starts to increase, because more particles enter the domain between the spheres with radii b and q . As this particle reaches $r = q$, the incoming and outgoing fluxes compensate each other and the entropy saturates.

The comparison of the entropies $S_m(R_\infty)$ (28) and $S_m(R_{\text{MS}})$ (31) is demonstrated in Fig. 9.

Islands of finite lifetime

Let us consider an arbitrary island configuration $I = [\mathbf{p}_-, \mathbf{a}_+]$, whose endpoints are parameterized as (see Fig. 10)

$$\mathbf{a}_+ = (a, t_a), \quad \mathbf{p}_- = \left(p, -t_p + \frac{i\pi}{\kappa_h} \right).$$

The full expression for $S_{\text{gen}}[I, R_{\text{MS}}]$ is given in Appendix A, formula (A6). Since it is symmetric under permutations of the island coordinates: $a \leftrightarrow p$, $t_a \leftrightarrow t_p$, the extremization equations for a and p , as well as for t_a and t_p , are the same. This fact tells us that we should consider a mirror-symmetric ansatz for the island

$$a = p, \quad t_a = t_p.$$

For intermediate times

$$\begin{aligned} \cosh \kappa_h (r_*(b) - r_*(a)) &\ll \cosh \kappa_h (t_a + t_b) \ll \\ &\ll \cosh \kappa_h (r_*(q) - r_*(a)), \end{aligned} \quad (34)$$

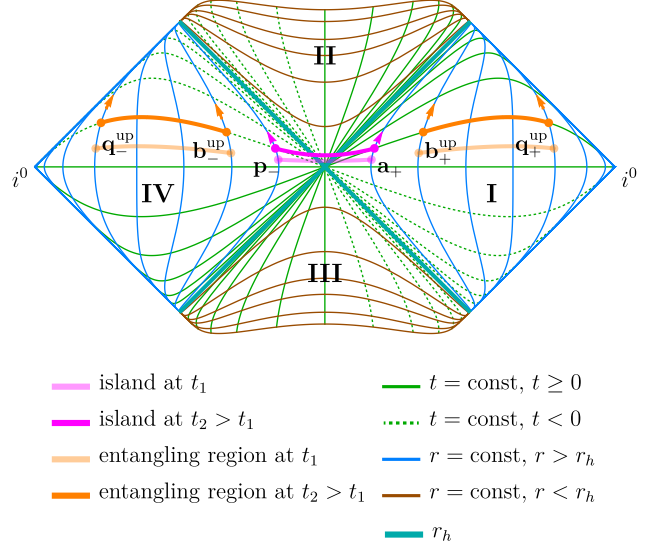


Figure 10. Penrose diagram for the eternal Schwarzschild black hole with a finite mirror-symmetric entangling region $R_{\text{MS}} \equiv [\mathbf{q}_-^{\text{up}}, \mathbf{b}_-^{\text{up}}] \cup [\mathbf{b}_+^{\text{up}}, \mathbf{q}_+^{\text{up}}]$ (orange) and the island $I = [\mathbf{p}_-, \mathbf{a}_+]$ (magenta). Arrows indicate the direction of flow of points during time evolution.

there is an analytical solution to the extremization equations

$$t_a = t_b, \quad 0 < a - r_h \ll r_h.$$

Using this, an approximate analytical expression for the entanglement entropy is given by (see Appendix (A17) for details)

$$\begin{aligned} S_{\text{gen}}^{\text{ext}}[I, R_{\text{MS}}] \Big|_{\text{inter. times}} &\simeq S(R_\infty) \Big|_{\text{late times}} + \frac{c}{3} \ln \cosh \kappa_h t_b - \\ &- \frac{c}{3} \exp \left[2\kappa_h t_b - \kappa_h (r_*(q) - r_*(b)) \right] + \frac{c}{6} \ln \frac{4f(q)}{\kappa_h^2 \varepsilon^2}. \end{aligned} \quad (35)$$

The first term on the RHS is the entropy for the semi-infinite region (29) studied in [18]. Other terms represent finite size effects. Interestingly, that the third term, being vanishingly small in the large- q limit, affects the dynamics, although its influence is suppressed at intermediate times. The fourth term gives the anomalous term (23) in the limit $q \rightarrow \infty$.

The growth of $S_{\text{gen}}^{\text{ext}}[I, R_{\text{MS}}]$ is approximately linear and is the same as of the entropy $S_m(R_\infty)$ (14), unlike $S_m(R_{\text{MS}})$ (32). The comparison with numerical results is shown in Fig. 11.

At early times

$$\cosh \kappa_h (t_a \pm t_b) \ll \cosh \kappa_h (r_*(b) - r_*(a)),$$

there is no real solution to the extremization problem for $a > r_h$, see (A11).

³ Since the eternal black hole radiates permanently, by the “first” particle of radiation we mean the referent one emitted at $t = 0$.

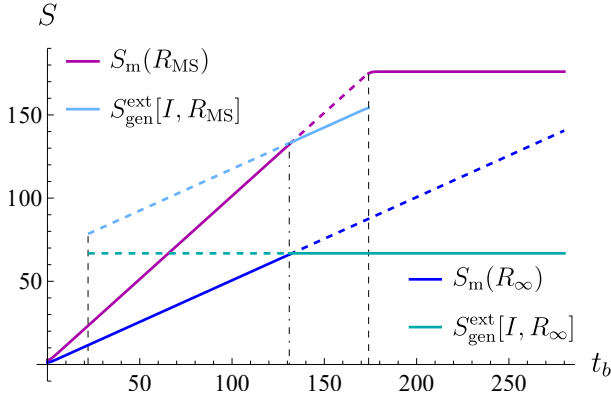


Figure 11. Entanglement entropy evolution of the finite entangling region R_{MS} with $q = 350$ (dark magenta, sky blue) and of the semi-infinite region R_{∞} (blue and cyan). For both cases, we take $b = 5$, $r_h = 1$, $c = 3$, $G_N = 0.1$, $\varepsilon = 1$. The dominating (minimum) contribution is marked with solid lines. Non-dominating configurations are marked with dashed lines. The moments of the emergence and disappearance of the islands are marked with black dashed lines. After the disappearance of the island for the region R_{MS} (sky blue), there is an instantaneous transition to the entropy for the configuration without island (dark magenta).

At late times

$$\begin{aligned} \cosh \kappa_h(t_a + t_b) &\gg \cosh \kappa_h(r_*(q) - r_*(a)), \\ \cosh 2\kappa_h t_b &\gg \cosh \kappa_h(r_*(q) - r_*(b)), \end{aligned}$$

along with $t_a \approx t_b$, the generalized entropy functional $S_{\text{gen}}[I, R_{\text{MS}}]$ grows monotonically with time t_a (A13), hence there is no solution either.

We conclude that the island exists only for a *finite time*, determined by the inequalities (34) (see Fig. 11). Starting from relatively small values of q , the island never dominates (see Fig. 12). Reducing the size of the finite region — by increasing b or decreasing q — leads to a decrease in the lifetime of the island (see Fig. 13). For sufficiently large b or small q , the island does not appear at all, i.e., there is a region size threshold, at which the island ceases to exist.

There is also a *discontinuity* in the entropy at the moment when the island disappears, see Fig. 11. In Section V, we will show that this behavior causes the entanglement entropy to exceed the Bekenstein-Hawking entropy.

Numerical analysis reveals several additional features. From Fig. 11 and 12, we note that the entropy for the configuration without islands reaches saturation at the moment that approximately coincides with the disappearance of the island. Also, the parameters of the island configuration a and t_a for R_{MS} coincides with that for R_{∞} , up to a short period of time before the disappearance of the island (see Fig. 14). The island gets smaller, but remains mirror-symmetric throughout the entire lifetime.

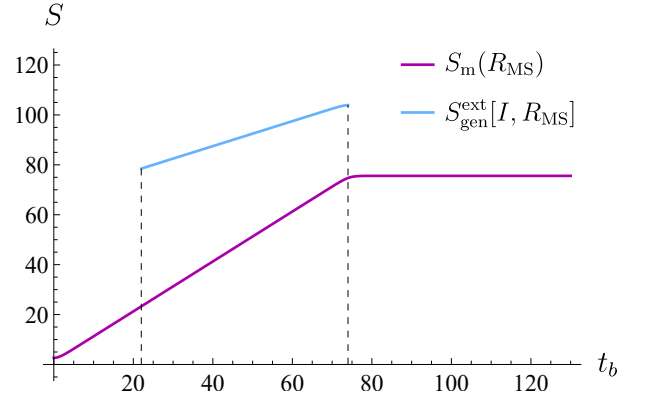


Figure 12. Entanglement entropy evolution of the region R_{MS} with $q = 150$ (dark magenta) and the generalized entanglement entropy functional $S_{\text{gen}}^{\text{ext}}[I, R_{\text{MS}}]$ (sky blue). We take the parameters as $b = 5$, $r_h = 1$, $c = 3$, $G_N = 0.1$, $\varepsilon = 1$. During the entire lifetime, the island does not dominate.

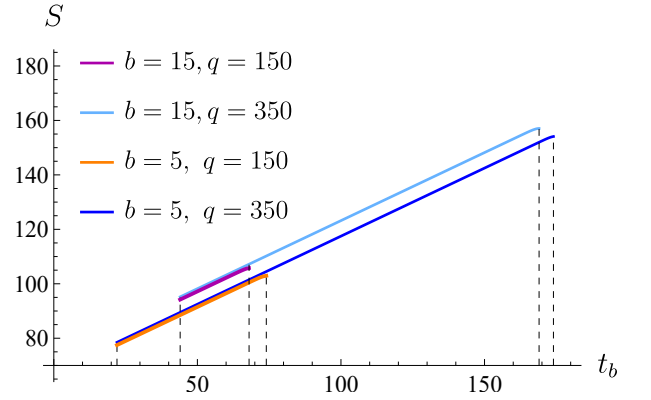


Figure 13. Time evolution of the generalized entanglement entropy $S_{\text{gen}}^{\text{ext}}[I, R_{\text{MS}}]$ for different b and q . The parameters are fixed as $r_h = 1$, $c = 3$, $G_N = 0.1$, $\varepsilon = 1$. A decrease in q leads to a faster disappearance of the island. An increase in b leads to its later appearance.

C. Asymmetric finite entangling region

Cauchy surface breaking

Now let us consider the following union of two intervals, which we call the *asymmetric (AS) finite entangling region* (see Fig. 15)

$$R_{\text{AS}} \equiv [\mathbf{q}_-^{\text{down}}, \mathbf{b}_-^{\text{up}}] \cup [\mathbf{b}_+^{\text{up}}, \mathbf{q}_+^{\text{up}}].$$

Its name comes from the fact that this region is not in any sense symmetrical in the Penrose diagram.

In this setup, there is an *upper bound* on time t_b (see Section IV A): during time evolution, the point $\mathbf{q}_-^{\text{down}}$ moves in time along the flow of the Killing vector ∂_t^- , while the point \mathbf{b}_-^{up} moves in the opposite direction, such that the interval between them eventually becomes time-like (see Fig. 15). Indeed, consider the distance squared

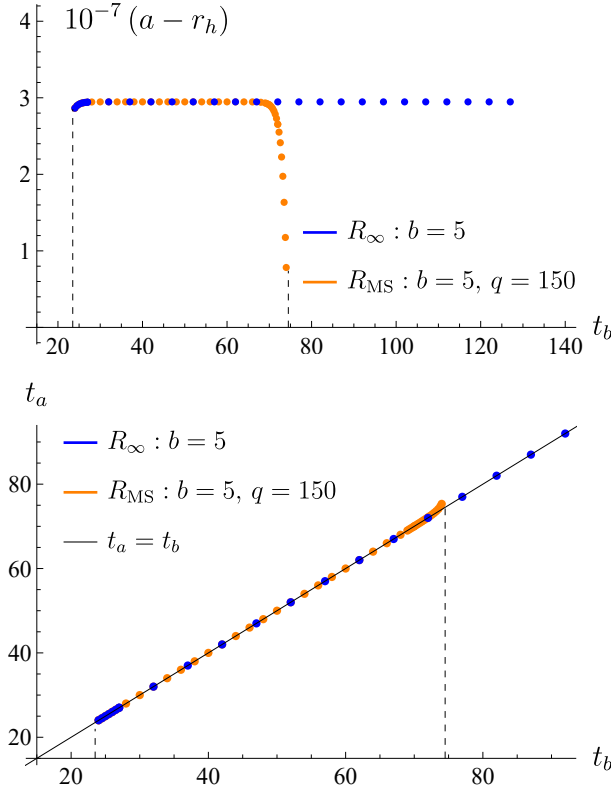


Figure 14. **Top:** Evolution of the island radial coordinate a corresponding to the finite size entangling region R_{MS} (orange) with $q = 150$, and to the semi-infinite region R_∞ (blue). **Bottom:** Evolution of the island time coordinate t_a for the same regions. Parameters are fixed as $b = 5$, $r_h = 1$, $c = 3$, $G_N = 0.1$, $\varepsilon = 1$. Just before the island for the region R_{MS} disappears, its coordinates start to deviate from the coordinates of the island for R_∞ .

between $\mathbf{q}_-^{\text{down}}$ and \mathbf{b}_-^{up}

$$d^2(\mathbf{q}_-^{\text{down}}, \mathbf{b}_-^{\text{up}}) \propto \cosh \kappa_h(r_*(q) - r_*(b)) - \cosh 2\kappa_h t_b.$$

This expression gets negative at the moment

$$t_{\text{break}}(b, q) = \frac{r_*(q) - r_*(b)}{2}. \quad (36)$$

Hence, for $t_b > t_{\text{break}}$, the problem becomes ill-defined, since there is no longer a Cauchy surface (i.e. a spacelike hypersurface) to define a pure quantum state. A larger size of the finite region R_{AS} leads to a larger t_{break} . In the limit $q \rightarrow \infty$, this time also gets infinite: $t_{\text{break}} \rightarrow \infty$, and the Cauchy surface breaking never happens.

For intermediate times $r_h \ll t_b \ll t_{\text{break}}$, the entanglement entropy for R_{AS} grows linearly (refer to Appendix (A18) for the full expression)

$$S_m(R_{AS}) \simeq \frac{c}{3} \kappa_h t_b. \quad (37)$$

Fig. 16 shows that the entanglement entropy for R_{AS} almost coincides with that for the semi-infinite region

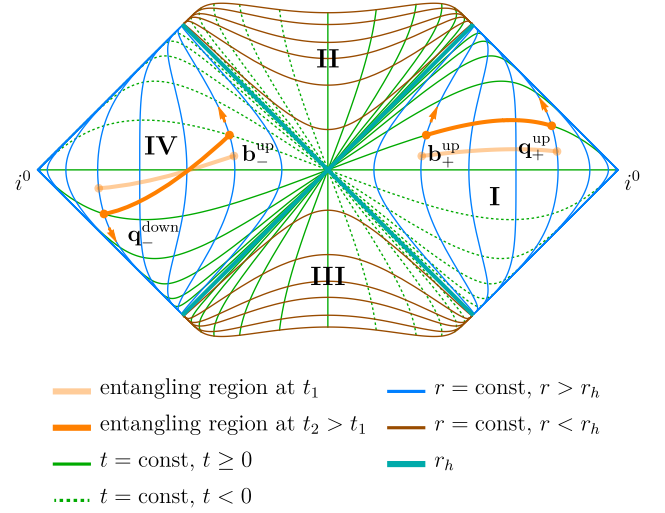


Figure 15. Penrose diagram for the eternal Schwarzschild black hole with a finite asymmetric entangling region $R_{AS} \equiv [\mathbf{q}_-^{\text{down}}, \mathbf{b}_-^{\text{up}}] \cup [\mathbf{b}_+^{\text{up}}, \mathbf{q}_+^{\text{up}}]$. Arrows indicate the direction of flow of points during time evolution.

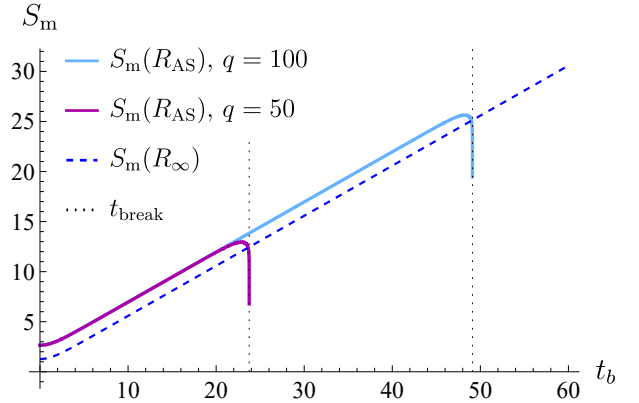


Figure 16. Entropy evolution for the finite entangling region R_{AS} with $q = 50$ (dark magenta), $q = 100$ (sky blue) and for the semi-infinite one R_∞ (blue). For all cases, we take $b = 5$, $r_h = 1$, $c = 3$, $\varepsilon = 1$. The entropy for R_{AS} has the same slope as that for R_∞ , but gets singular at t_{break} (36) (dotted lines).

R_∞ , without strong dependence on q . Just before the breaking time t_{break} , the entropy abruptly decreases and hits the singularity, after which it is not well-defined.

Non-symmetric islands

Let us consider the island ansatz $I = [\mathbf{p}_-, \mathbf{a}_+]$ for the AS entangling region (see Fig. 17). For relatively early times, i.e.

$$\begin{aligned} \cosh \kappa_h(t_p + t_b) &\ll \cosh \kappa_h(r_*(q) - r_*(p)), \\ \cosh \kappa_h(t_a - t_b) &\ll \cosh \kappa_h(r_*(q) - r_*(a)), \end{aligned}$$

all the terms in the formula for the generalized entropy functional $S_{\text{gen}}[I, R_{\text{AS}}]$, that are non-symmetric with respect to permutations of the island coordinates: $a \leftrightarrow p$, $t_a \leftrightarrow t_p$, get suppressed (see Appendix (A20)). Hence, for early times, it is reasonable to take a mirror-symmetric ansatz: $a \simeq p$, $t_a \simeq t_p$.

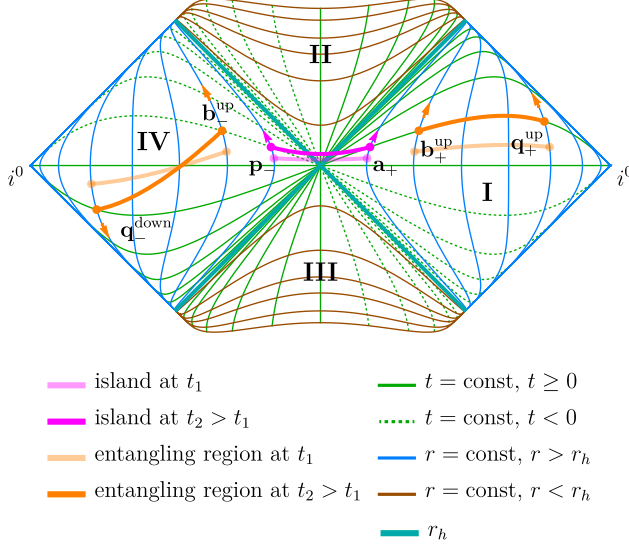


Figure 17. Penrose diagram for the eternal Schwarzschild black hole with a finite asymmetric entangling region $R_{\text{AS}} \equiv [\mathbf{q}_{-}^{\text{down}}, \mathbf{b}_{-}^{\text{up}}] \cup [\mathbf{b}_{+}^{\text{up}}, \mathbf{q}_{+}^{\text{up}}]$ (orange) and the island $I = [\mathbf{p}_{-}, \mathbf{a}_{+}]$ (magenta). Arrows indicate the direction of flow of points during time evolution.

Then, for intermediate times

$$\begin{aligned} \cosh \kappa_h(r_*(a) - r_*(b)) &\ll \cosh \kappa_h(t_a + t_b) \ll \\ &\ll \cosh \kappa_h(r_*(q) - r_*(b)), \end{aligned} \quad (38)$$

the extremization gives the same solution as in [18]

$$t_a = t_b, \quad 0 < a - r_h \ll r_h.$$

The approximate analytical expression for the generalized entropy is given by (A26)

$$\begin{aligned} S_{\text{gen}}^{\text{ext}}[I, R_{\text{AS}}] \Big|_{\text{inter. times}} &\simeq S(R_{\infty}) \Big|_{\text{late times}} - \\ &- \frac{c}{3} \exp \left[2\kappa_h t_b - \kappa_h(r_*(q) - r_*(b)) \right] + \frac{c}{6} \ln \frac{4f(q)}{\kappa_h^2 \varepsilon^2}. \end{aligned} \quad (39)$$

The limit $q \rightarrow \infty$ at fixed t_b of this expression recovers the semi-infinite case (29), except for the anomalous term (23), which is to be subtracted.

At late times

$$\begin{aligned} \cosh \kappa_h(t_p + t_b) &\gg \cosh \kappa_h(r_*(q) - r_*(p)), \\ \cosh \kappa_h(t_a - t_b) &\gg \cosh \kappa_h(r_*(q) - r_*(a)), \end{aligned}$$

the contribution of non-symmetric terms in $S_{\text{gen}}[I, R_{\text{AS}}]$ becomes significant, which leads to the fact that the

solution to the extremization equations becomes non-symmetric. This logic is verified by numerical calculations, see Fig. 18.

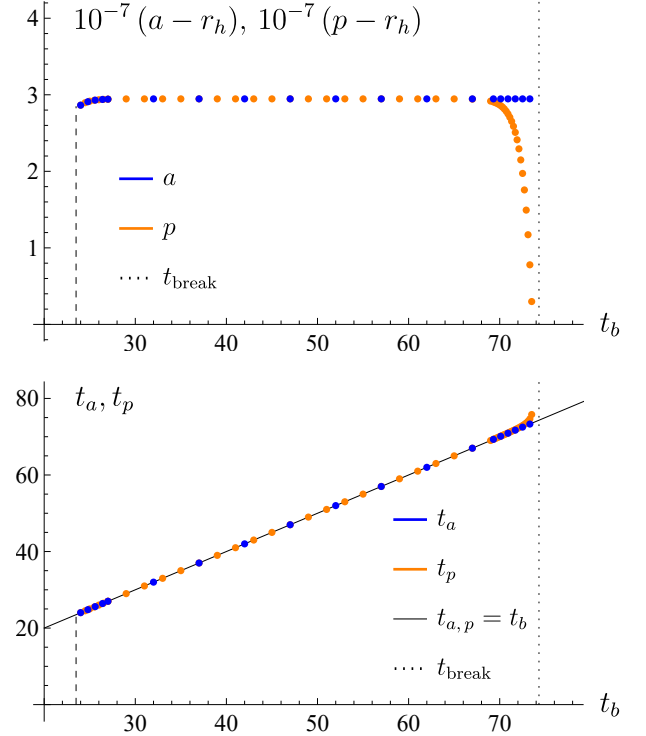


Figure 18. **Top:** Evolution of the island radial coordinates a (blue) and p (orange) corresponding to the finite size entangling region R_{AS} with $b = 5$, $q = 150$. **Bottom:** Evolution of the island time coordinates t_a (blue) and t_p (orange) corresponding to the same region. Parameters are fixed as $r_h = 1$, $c = 3$, $G_N = 0.1$, $\varepsilon = 1$. Near the breaking time t_{break} (36), there is spatial $a \neq p$ and time $t_a \neq t_p$ asymmetries.

Numerical results provide us with more details. For large finite entangling regions $r_*(q) \gg r_*(b)$ (see Fig. 19), the dynamics of the entropy is qualitatively the same as for R_{∞} , except that $S(R_{\text{AS}})$ slightly decreases just before the Cauchy surface breaking. For smaller regions, the island contribution is never dominant (see Fig. 20).

The Cauchy surface breaking, which bounds the lifetime of the configuration containing AS finite region, constrains the lifetime of the island as well. It is not the case for sufficiently large regions, such that $\cosh \kappa_h(r_*(a) - r_*(b)) \ll \cosh \kappa_h t_{\text{break}}$, because in this case, there is no solution under the condition (38). However, for smaller regions, the appearance of the island may not occur before t_{break} .

The lifetime of the island shortens as the size of the entangling region R_{AS} gets smaller (as q decreases or b increases, see Fig. 21).

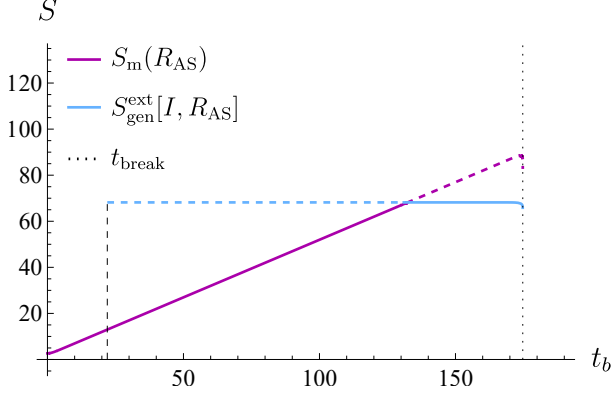


Figure 19. Entanglement entropy evolution of the region R_{AS} with $b = 5$ and $q = 350$ (dark magenta), and of the same region with the island (sky blue). The parameters are taken as $r_h = 1$, $c = 3$, $G_N = 0.1$ and $\varepsilon = 1$. Note the abrupt decrease near t_{break} (36), which is caused by the subsequent Cauchy surface breaking.

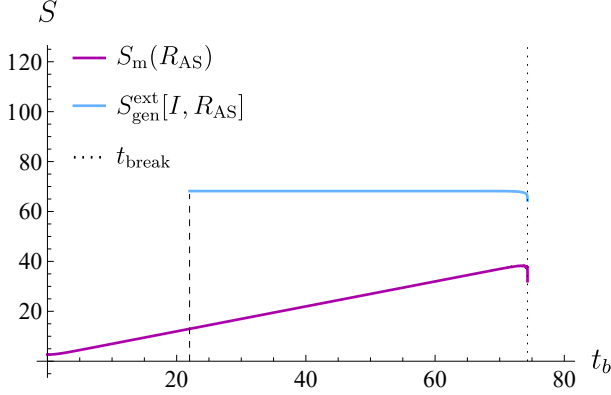


Figure 20. Entanglement entropy evolution of the region R_{AS} with $b = 5$ and $q = 150$ (dark magenta), and of the same region with the island (sky blue). The parameters are taken as $r_h = 1$, $c = 3$, $G_N = 0.1$ and $\varepsilon = 1$. The extremization procedure never leads us the entropy with an island over that for the configuration without island.

V. INFORMATION LOSS PARADOX FOR FINITE ENTANGLING REGIONS

A Cauchy surface Σ in the eternal Schwarzschild black hole might be divided into the semi-infinite entangling region R_∞ , the region associated with the black hole BH , and the domain in-between. If the latter is negligible, we have

$$\Sigma = BH \cup R_\infty. \quad (40)$$

Given that the state is pure, the entanglement entropy obeys the complementarity property

$$S(R_\infty) = S(BH). \quad (41)$$

The fine-grained entropy $S(BH)$ is to be bounded from

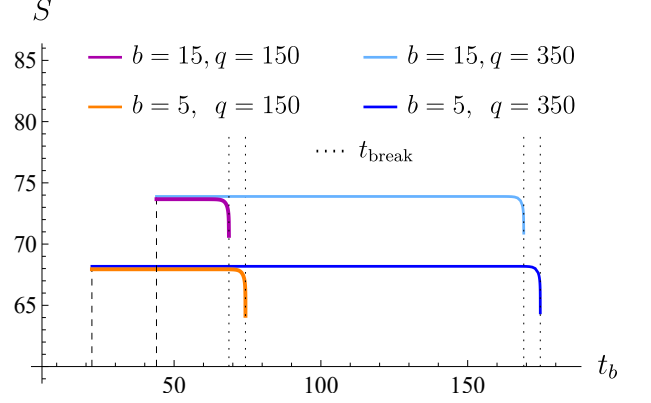


Figure 21. Time evolution of the generalized entanglement entropy $S_{\text{gen}}^{\text{ext}}[I, R_{AS}]$ for different b and q . Parameters are fixed as $r_h = 1$, $c = 3$, $G_N = 0.1$, $\varepsilon = 1$. The lifetime of the island configuration increases due to the change in the time of the Cauchy surface breaking t_{break} , as well as due to the dependence of the time of the island appearance on b .

above by the coarse-grained entropy $S_{\text{thermo}}(BH)$

$$S(BH) \leq S_{\text{thermo}}(BH). \quad (42)$$

The latter is twice the Bekenstein-Hawking entropy [12, 18]

$$S_{\text{thermo}}(BH) = 2S_{B-H} = \frac{2\pi r_h^2}{G_N}. \quad (43)$$

As a result, the upper bound on the entanglement entropy of Hawking radiation is expected to be [25]

$$S(R_\infty) \leq 2S_{B-H}. \quad (44)$$

In fact, this limit is violated due to the unstoppable growth of the entanglement entropy. This might be seen as a version of the information loss paradox [12, 18].

The evolution of the entropy changes in the presence of entanglement islands. When the island starts to dominate, the entanglement entropy is given by (29) and consists of two terms, one of which is the Bekenstein-Hawking entropy, while the other denotes additional corrections

$$S(R_\infty) \Big|_{\text{late times}} \simeq 2S_{B-H} + S_{\text{corr}}. \quad (45)$$

These corrections are time-independent and small compared to the area term S_{B-H} under the “black hole classicality” condition [18]

$$\frac{r_h^2}{G_N} \gg c. \quad (46)$$

We say that the information paradox in two-sided Schwarzschild black hole does not arise if either the bound (44) is respected or violated only by terms suppressed under (46). Formally,

$$S(R_\infty) \leq 2S_{B-H} + S_{\text{corr}}, \quad \frac{S_{\text{corr}}}{S_{B-H}} \ll 1. \quad (47)$$

We can also divide a Cauchy surface into the region associated with the black hole BH , a finite entangling region R , a finite domain in-between and an adjacent semi-infinite region C , which extends to spacelike infinities i^0 (see Fig. 22)

$$\Sigma = BH \cup R \cup C. \quad (48)$$

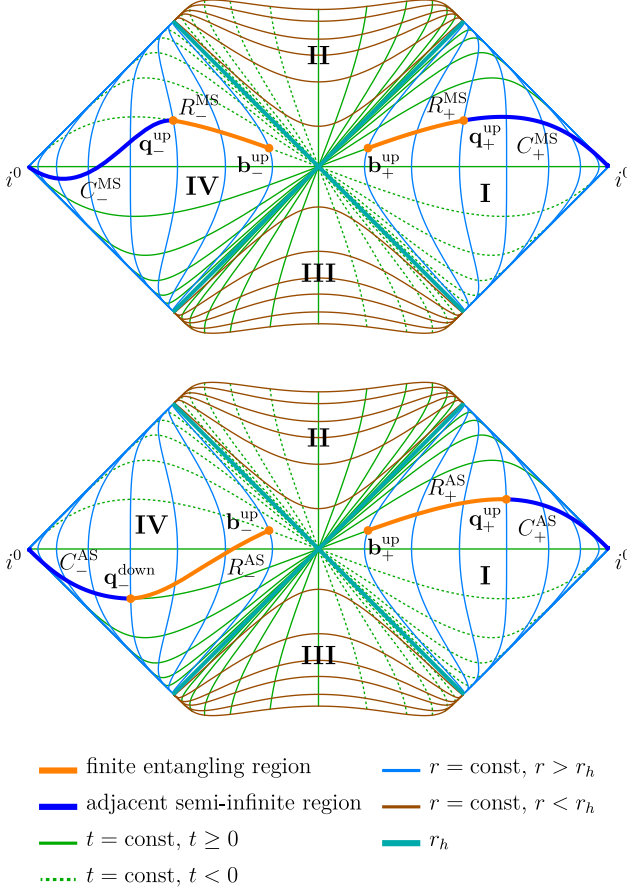


Figure 22. **Top:** Penrose diagram for the eternal Schwarzschild black hole with semi-infinite entangling region R_∞ partitioned into finite MS subregion, $R_{\text{MS}} \equiv R_-^{\text{MS}} \cup R_+^{\text{MS}}$ (orange), and its adjacent semi-infinite region $C_{\text{MS}} \equiv C_-^{\text{MS}} \cup C_+^{\text{MS}}$ (blue). **Bottom:** The same diagram with semi-infinite entangling region R_∞ partitioned into finite AS subregion, $R_{\text{AS}} \equiv R_-^{\text{AS}} \cup R_+^{\text{AS}}$ (orange), and its adjacent semi-infinite region $C_{\text{AS}} \equiv C_-^{\text{AS}} \cup C_+^{\text{AS}}$ (blue).

The strong subadditivity of entanglement entropy [78] for a tripartition like (48) gives the inequality

$$S(BH \cup R \cup C) + S(R) \leq S(BH \cup R) + S(R \cup C). \quad (49)$$

Then, using the complementarity property

$$\begin{aligned} S(BH) &= S(R \cup C), \\ S(R) &= S(BH \cup C), \\ S(C) &= S(BH \cup R), \end{aligned} \quad (50)$$

and pure state condition for the total state, $S(\Sigma) = 0$, we derive the upper bound on the entanglement entropy for a finite region R (*the strong bound*)

$$S(R) \leq 2S_{\text{B-H}} + S(C). \quad (51)$$

We interpret its violation as the information paradox for finite entangling regions. The island prescription leads to softening of this constraint (*the soft bound*)

$$S(R) \leq 2S_{\text{B-H}} + S(C) + S_{\text{corr}}. \quad (52)$$

A. MS finite entangling region

Do islands for C_{MS} influence the bound?

As C_{MS} we referred to a semi-infinite outer entangling region, which is adjacent to R_{MS} . It can be defined as the limit of the following finite entangling region

$$C_{\text{MS}} = \lim_{w \rightarrow \infty} [\mathbf{w}_-^{\text{down}}, \mathbf{q}_-^{\text{up}}] \cup [\mathbf{q}_+^{\text{up}}, \mathbf{w}_+^{\text{up}}].$$

The points $\mathbf{w}_-^{\text{down}}$ and \mathbf{w}_+^{up} are IR regulators. Essentially, it is the same region as considered in [18]. Hence, we already know the features of its dynamics: the entropy for C_{MS} grows at early times (see (14))

$$S(C_{\text{MS}})|_{\text{early times}} = \frac{c}{6} \ln \left(\frac{4f(q) \cosh^2 \kappa_h t_q}{\kappa_h^2 \varepsilon^2} \right), \quad (53)$$

while at late times, it saturates due to the formation of the island I_C for this region (see (29))

$$S(C_{\text{MS}})|_{\text{late times}} \simeq \frac{2\pi r_h^2}{G_{\text{N}}} + \frac{c}{6} \ln \frac{f(q)}{\kappa_h^4 \varepsilon^4} + \frac{c}{6} (2\kappa_h r_*(q) - 1). \quad (54)$$

Since the endpoints $\mathbf{q}_\pm^{\text{up}}$ are adjacent for R_{MS} and C_{MS} , their shifts influence oppositely the formation of the islands I for R_{MS} and I_C for C_{MS} . Indeed, there are the island solutions, when the following conditions are satisfied

$$\begin{aligned} R_{\text{MS}}: & \cosh \kappa_h (r_*(b) - r_*(a^R)) \ll \cosh \kappa_h (t_a^R + t_b) \ll \\ & \ll \cosh \kappa_h (r_*(q) - r_*(a^R)), \\ C_{\text{MS}}: & \cosh \kappa_h (t_a^C + t_b) \gg \cosh \kappa_h (r_*(q) - r_*(a^C)) > \\ & > \cosh \kappa_h (r_*(q) - r_*(b)). \end{aligned}$$

We see that these conditions cannot hold together because $a^R \simeq a^C$, therefore, the corresponding islands I and I_C do not exist simultaneously.

Actually, even when the island I_C is formed, the bound on the entropy for R_{MS} , imposed by $S(C_{\text{MS}})|_{\text{late times}}$, cannot be violated, because $S(C_{\text{MS}})|_{\text{late times}}$ (54) and $S_{\text{m}}(R_{\text{MS}})|_{\text{late times}}$ (33) have the same dependence on q , thus never intersect. What we are left with to check is whether

the strong bound, related to C_{MS} without the island I_C , holds

$$S(R_{\text{MS}}) \stackrel{?}{\leq} S_{\text{bound}} = \frac{2\pi r_h^2}{G_N} + \frac{c}{6} \ln \left(\frac{4f(q) \cosh^2 \kappa_h t_q}{\kappa_h^2 \varepsilon^2} \right). \quad (55)$$

Without islands for R_{MS}

Since the entropy of matter for MS region (32) grows twice as fast as that for the semi-infinite region R_∞ , and the strong bound (55) is imposed by the semi-infinite region of the same type as R_∞ , the bound might be eventually violated. However, the entropy saturates at some finite value (see Section IV B), while the bound would keep growing linearly. Therefore, if the bound is violated, then only for a finite time (see dark magenta curve in Fig. 23).

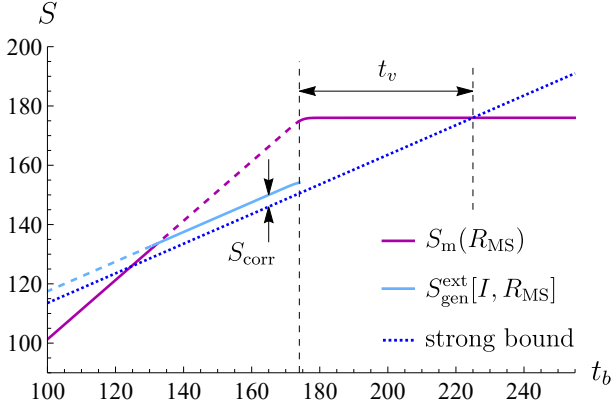


Figure 23. The early-time evolution of the matter entropy $S_m(R_{\text{MS}})$ (dark magenta), the entropy for the configuration with the island $S_{\text{gen}}^{\text{ext}}[I, R_{\text{MS}}]$ (sky blue) and the strong bound (55) (dotted blue) for a finite size entangling region R_{MS} with $b = 5$ and $q = 350$. We take $r_h = 1$, $c = 3$, $G_N = 0.1$, $\varepsilon = 1$. After the disappearance of the island, there is a discontinuous transition to the entropy of matter $S_m(R_{\text{MS}})$ that is larger than the upper bound during some finite time of violation t_v . As q increases, the maximum difference between $S_m(R_{\text{MS}})$ and the strong bound increases, while S_{corr} does not change significantly.

Island dominating for finite time

When the island I dominates, $S_{\text{gen}}^{\text{ext}}[I, R_{\text{MS}}]$ is larger than the strong bound by S_{corr} , which does not change significantly if we vary q . Indeed, their difference S_{corr} is

$$\begin{aligned} S_{\text{corr}} &= S_{\text{gen}}^{\text{ext}}[I, R_{\text{MS}}] - S_{\text{bound}} \simeq \\ &\simeq \frac{c}{6} \ln \frac{f(b)}{\kappa_h^4 \varepsilon^4} + \frac{c}{3} \kappa_h r_*(b) - \frac{c}{6} - \\ &\quad - \frac{c}{3} \exp \left[2\kappa_h t_b - \kappa_h (r_*(q) - r_*(b)) \right], \end{aligned} \quad (56)$$

with a strongly suppressed dependence on t_b and q .

After the disappearance of the island, there is a discontinuous transition to the constant entropy (33). Its value depends on q and is significantly larger than the strong bound (see Fig. 23), because during the island domination, the matter entropy $S_m(R_{\text{MS}})$ grows twice as fast (32) as the bound. After that, the difference decreases. The larger the value of q is — the longer the constraint is violated. Thus, we say that the island prescription for R_{MS} does *not* solve the information paradox completely.

Never dominant island

For relatively small sizes of the region R_{MS} , the entropy of matter always dominates (see Section IV B) and does not exceed the entropy with an island

$$S(R_{\text{MS}}) = S_m(R_{\text{MS}}) < S_{\text{gen}}^{\text{ext}}[I, R_{\text{MS}}] = S_{\text{bound}} + S_{\text{corr}}, \quad (57)$$

hence, the soft bound is not violated.

B. AS finite entangling region

The semi-infinite adjacent region for AS region turns out to be neither of MS type nor AS. It can be defined as the following limit

$$C_{\text{AS}} = \lim_{w \rightarrow \infty} [\mathbf{w}_-^{\text{down}}, \mathbf{q}_-^{\text{down}}] \cup [\mathbf{q}_+^{\text{up}}, \mathbf{w}_+^{\text{up}}].$$

The entropy of matter for this region is (see Appendix (A27))

$$S_m(C_{\text{AS}}) = \frac{c}{6} \ln \frac{4f(q)}{\kappa_h^2 \varepsilon^2}, \quad (58)$$

which is time-independent, because all points of C_{AS} lie on the same timeslice. This entropy is of order of $c \ll r_h^2/G_N$, and hence, it is subdominant compared to $S_{\text{B-H}}$. This means that there is no information paradox for the region C_{AS} even without islands.

As for the region R_{AS} , the strong bound (51) is explicitly given by

$$S(R_{\text{AS}}) \stackrel{?}{\leq} S_{\text{bound}} = \frac{2\pi r_h^2}{G_N} + \frac{c}{6} \ln \frac{4f(q)}{\kappa_h^2 \varepsilon^2}. \quad (59)$$

We want to check whether this inequality holds.

Without islands

If we do not take into account the islands for R_{AS} , the entanglement entropy for R_{AS} has the largest possible value just before the Cauchy surface breaking. For large enough q , the entropy exceeds the strong bound (see dark magenta curve in Fig. 24). However, there is some critical

value q_{crit} , such that for $q < q_{\text{crit}}$ the Cauchy surface breaks before the strong bound is violated, and hence, the information paradox does not arise.

Island dominating for finite time

The island contribution to the generalized entropy $S(R_{\text{AS}})$ starts to dominate for large enough q . It exceeds the strong bound (51) (see Fig. 24), but the soft bound is still satisfied

$$S(R_{\text{AS}}) \leq S_{\text{bound}} + S_{\text{corr}}, \quad (60)$$

where $S_{\text{corr}} = S_{\text{gen}}^{\text{ext}}[I, R_{\text{AS}}] - S_{\text{bound}}$ is given by the same expression as in the MS case (56) and is proportional to $c \ll r_h^2/G_N$.

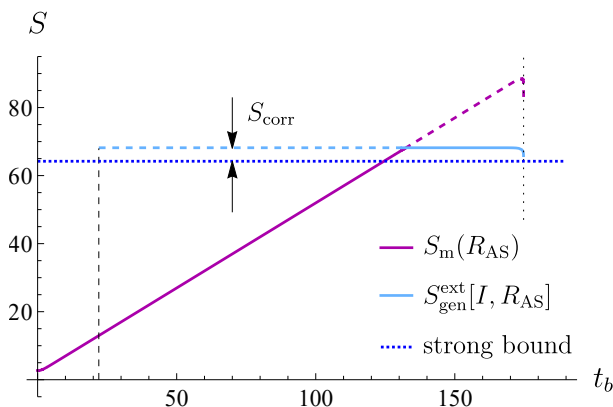


Figure 24. Time evolution of the entropy $S_m(R_{\text{AS}})$ (dark magenta), the generalized entropy $S_{\text{gen}}^{\text{ext}}[I, R_{\text{AS}}]$ (sky blue) and the strong bound (59) (dotted blue) for the finite size entangling region R_{MS} with $b = 5$ and $q = 350$. The parameters are $r_h = 1$, $c = 3$, $G_N = 0.1$, $\varepsilon = 1$. Introduction of the island helps to keep the entropy close to the bound within the level of corrections S_{corr} .

Never dominant island

If the island configuration never dominates, then the entropy of matter is always less than the generalized entropy

$$S(R_{\text{AS}}) = S_m(R_{\text{AS}}) < S_{\text{gen}}^{\text{ext}}[I, R_{\text{AS}}] = S_{\text{bound}} + S_{\text{corr}}. \quad (61)$$

Therefore, the soft bound (52) is obeyed.

VI. CONCLUSIONS AND FUTURE PROSPECTS

In this paper, we address the properties of the entanglement entropy of Hawking radiation on the background of the eternal Schwarzschild black hole in the case of

entangling regions of finite size. This can be seen as a starting point for studying the entropy in spacetimes with finite observable domains. Among them are de Sitter (dS) and Schwarzschild-de Sitter (SdS) universes, where a physical observer is bounded within the cosmological horizon. Therefore, only finite entangling regions are of physical significance in these spacetimes, and a generalization of the results of this paper on dS and SdS cases is needed.

We have elaborated on the infrared regularization of spacelike infinities of Cauchy surfaces and semi-infinite regions in two-sided Schwarzschild spacetime. Our procedure allows complementarity and pure state condition to be satisfied explicitly in direct calculations in the prescription of subtracting the anomalous term.

We have established two qualitatively different types of finite entangling regions — mirror-symmetric (MS) and asymmetric (AS). The first type represents finite domains between concentric spheres. The slope of the early-time evolution of the entanglement entropy of conformal matter for such regions is twice as large as for the canonical semi-infinite setup. For late times, the entropy saturates at a constant value even without entanglement islands. Island configurations exist only for finite time for such regions.

The outer endpoints of AS regions are chosen spatially symmetric and lie on the same timeslice. The corresponding Cauchy surfaces have a finite lifetime depending on the size of the entangling regions. In this case, one gets a linear growth of the entropy with time. At the time when the Cauchy surface breaks, the entanglement entropy hits singularity. Just before this moment, the island configuration gets non-symmetric. Also, islands for the regions of both types might never dominate in the generalized entropy functional if their size is relatively small.

We have derived constraints from above on the entanglement entropy for finite entangling regions coming from strong subadditivity and complementarity. The upper bounds depend on the size of the region and on the location of its endpoints. For the AS type, the paradox is solved by entanglement islands. However, the entanglement entropy for MS regions might violate the upper bound even in the island prescription.

ACKNOWLEDGMENTS

We would like to thank M. Khramtsov and I. Volovich for useful discussions. DA, IA and TR are supported by the Russian Science Foundation (project 20-12-00200, Steklov Mathematical Institute).

Appendix A: Explicit formulas for entanglement entropy for finite entangling regions

1. MS entangling region without island

With use of the formula for the entropy collected in multiple intervals (9) and the formula for distances (8), along with the definition of up- and down- points (30), the entanglement entropy for the mirror-symmetric finite entangling region takes the form

$$\begin{aligned}
S(R_{\text{MS}}) &= \frac{c}{3} \ln \left(\frac{d(\mathbf{b}_+^{\text{up}}, \mathbf{b}_-^{\text{up}}) d(\mathbf{q}_-^{\text{up}}, \mathbf{b}_+^{\text{up}})}{\varepsilon^2} \right) + \\
&+ \frac{c}{3} \ln \left(\frac{d(\mathbf{b}_+^{\text{up}}, \mathbf{q}_+^{\text{up}}) d(\mathbf{q}_-^{\text{up}}, \mathbf{q}_+^{\text{up}})}{\varepsilon^2} \right) - \\
&- \frac{c}{3} \ln \left(\frac{d(\mathbf{b}_-^{\text{up}}, \mathbf{q}_+^{\text{up}}) d(\mathbf{q}_-^{\text{up}}, \mathbf{b}_+^{\text{up}})}{\varepsilon^2} \right) = \\
&= \frac{c}{6} \ln \left[\frac{16f(b)f(q)}{\kappa_h^4 \varepsilon^4} \cosh^4 \kappa_h t_b \right] + \\
&+ \frac{c}{3} \ln \left[\frac{\cosh \kappa_h(r_*(q) - r_*(b)) - 1}{\cosh \kappa_h(r_*(q) - r_*(b)) + \cosh 2\kappa_h t_b} \right]. \tag{A1}
\end{aligned}$$

At late times, such that

$$\cosh 2\kappa_h t_b \gg \cosh \kappa_h(r_*(q) - r_*(b)), \tag{A2}$$

the expression simplifies to

$$\begin{aligned}
S(R_{\text{MS}}) \Big|_{\text{late times}} &\simeq \frac{c}{6} \ln \left(\frac{16f(b)f(q)}{\kappa_h^4 \varepsilon^4} \right) + \\
&+ \frac{c}{3} \ln [\cosh \kappa_h(r_*(q) - r_*(b)) - 1]. \tag{A3}
\end{aligned}$$

In the limit $q \rightarrow \infty$, we get

$$\lim_{q \rightarrow \infty} S(R_{\text{MS}}) = \frac{c}{6} \ln \left(\frac{16f(b)}{\kappa_h^4 \varepsilon^4} \cosh^4(\kappa_h t_b) \right). \tag{A4}$$

2. MS entangling region with island

The entropy for a non-trivial island configuration before the extremization procedure has the form (10). A general single-interval, non-symmetric ansatz for the island is $I = [\mathbf{p}_-, \mathbf{a}_+]$. The area of its boundary is

$$\text{Area}(\partial I) = 4\pi (a^2 + p^2). \tag{A5}$$

With use of this, the entanglement entropy functional takes the form

$$\begin{aligned}
S_{\text{gen}}[I, R_{\text{MS}}] &= \frac{\pi(a^2 + p^2)}{G_{\text{N}}} + \\
&+ \frac{c}{6} \ln \left[\frac{32\sqrt{f(a)f(p)}f(b)f(q)}{\kappa_h^6 \varepsilon^6} \cosh^4 \kappa_h t_b \right] + \\
&+ \frac{c}{6} \ln [\cosh \kappa_h(r_*(a) - r_*(p)) + \cosh \kappa_h(t_a + t_p)] + \\
&+ \frac{c}{6} \ln \left[\frac{\cosh \kappa_h(r_*(b) - r_*(a)) - \cosh \kappa_h(t_a - t_b)}{\cosh \kappa_h(r_*(b) - r_*(a)) + \cosh \kappa_h(t_a + t_b)} \right] + \\
&+ \frac{c}{6} \ln \left[\frac{\cosh \kappa_h(r_*(b) - r_*(p)) - \cosh \kappa_h(t_p - t_b)}{\cosh \kappa_h(r_*(b) - r_*(p)) + \cosh \kappa_h(t_p + t_b)} \right] + \\
&+ \frac{c}{6} \ln \left[\frac{\cosh \kappa_h(r_*(q) - r_*(a)) + \cosh \kappa_h(t_a + t_b)}{\cosh \kappa_h(r_*(q) - r_*(a)) - \cosh \kappa_h(t_a - t_b)} \right] + \\
&+ \frac{c}{6} \ln \left[\frac{\cosh \kappa_h(r_*(q) - r_*(p)) + \cosh \kappa_h(t_p + t_b)}{\cosh \kappa_h(r_*(q) - r_*(p)) - \cosh \kappa_h(t_p - t_b)} \right] + \\
&+ \frac{c}{3} \ln \left[\frac{\cosh \kappa_h(r_*(q) - r_*(b)) - 1}{\cosh \kappa_h(r_*(q) - r_*(b)) + \cosh 2\kappa_h t_b} \right]. \tag{A6}
\end{aligned}$$

This expression is to be extremized with respect to the parameters (a, t_a, p, t_p) .

The four-parameter extremization can be brought to extremization over only two parameters. Indeed, all the terms in $S_{\text{gen}}[I, R_{\text{MS}}]$ are symmetric with respect to permutations $a \leftrightarrow p$, $t_a \leftrightarrow t_p$, hence, it is reasonable to take a mirror-symmetric ansatz for the island, $I_{\text{MS}} = [\mathbf{a}_-, \mathbf{a}_+]$. For such a choice, the full expression for the generalized entropy functional reads as

$$\begin{aligned}
S_{\text{gen}}[I_{\text{MS}}, R_{\text{MS}}] &= \frac{2\pi a^2}{G_{\text{N}}} + \\
&+ \frac{c}{6} \ln \left[\frac{64f(a)f(b)f(q)}{\kappa_h^6 \varepsilon^6} \cosh^2 \kappa_h t_a \cosh^4 \kappa_h t_b \right] + \\
&+ \frac{c}{3} \ln \left[\frac{\cosh \kappa_h(r_*(b) - r_*(a)) - \cosh \kappa_h(t_a - t_b)}{\cosh \kappa_h(r_*(b) - r_*(a)) + \cosh \kappa_h(t_a + t_b)} \right] + \\
&+ \frac{c}{3} \ln \left[\frac{\cosh \kappa_h(r_*(q) - r_*(a)) + \cosh \kappa_h(t_a + t_b)}{\cosh \kappa_h(r_*(q) - r_*(a)) - \cosh \kappa_h(t_a - t_b)} \right] + \\
&+ \frac{c}{3} \ln \left[\frac{\cosh \kappa_h(r_*(q) - r_*(b)) - 1}{\cosh \kappa_h(r_*(q) - r_*(b)) + \cosh 2\kappa_h t_b} \right]. \tag{A7}
\end{aligned}$$

In this expression, we can identify a part of the terms with the generalized entropy functional for the semi-infinite region and the other part with an effect of finite size of the region,

$$\begin{aligned}
S_{\text{gen}}[I_{\text{MS}}, R_{\text{MS}}] &= S_{\text{gen}}[I_{\text{MS}}, R_{\infty}] + \\
&+ \frac{c}{6} \ln \left[\frac{4f(q)}{\kappa_h^2 \varepsilon^2} \cosh^2 \kappa_h t_b \right] + \\
&+ \frac{c}{3} \ln \left[\frac{\cosh \kappa_h(r_*(q) - r_*(a)) + \cosh \kappa_h(t_a + t_b)}{\cosh \kappa_h(r_*(q) - r_*(a)) - \cosh \kappa_h(t_a - t_b)} \right] + \\
&+ \frac{c}{3} \ln \left[\frac{\cosh \kappa_h(r_*(q) - r_*(b)) - 1}{\cosh \kappa_h(r_*(q) - r_*(b)) + \cosh 2\kappa_h t_b} \right]. \tag{A8}
\end{aligned}$$

It can be simplified further by using small-, intermediate- or large-time approximations.

We use a general property that for $x \gg 1$ holds $\cosh x \simeq \frac{1}{2}e^x$, and for A and B such that $\cosh B \ll \cosh A$ and $A \gg 1$ holds

$$\ln(\cosh A + \cosh B) \approx A + 2 \cosh B \exp(-A). \quad (\text{A9})$$

Then, for early times (small with respect to tortoise radial coordinate of the inner endpoints),

$$\begin{aligned} \cosh \kappa_h(t_a \pm t_b) &\ll \cosh \kappa_h(r_*(b) - r_*(a)) < \\ &< \cosh \kappa_h(r_*(q) - r_*(a)), \end{aligned} \quad (\text{A10})$$

we obtain

$$\begin{aligned} S_{\text{gen}}[I_{\text{MS}}, R_{\text{MS}}] \Big|_{\text{early times}} &\simeq S_{\text{gen}}[I_{\text{MS}}, R_{\infty}] + \\ &+ \frac{c}{6} \ln \left(\frac{4f(q)}{\kappa_h^2 \varepsilon^2} \cosh^2 \kappa_h t_b \right). \end{aligned} \quad (\text{A11})$$

Since the remaining term, describing the effect of the finite size of the region, does not depend neither on a nor t_a , there is no solution as in the semi-infinite case [18].

For late times

$$\begin{aligned} \cosh \kappa_h(t_a + t_b) &\gg \cosh \kappa_h(r_*(q) - r_*(a)), \\ \cosh 2\kappa_h t_b &\gg \cosh \kappa_h(r_*(q) - r_*(b)), \end{aligned} \quad (\text{A12})$$

the functional reduces to

$$\begin{aligned} S_{\text{gen}}[I_{\text{MS}}, R_{\text{MS}}] \Big|_{\text{late times}} &\simeq \frac{2\pi a^2}{G_N} + \\ &+ \frac{c}{3} \kappa_h(t_a + t_b) + \frac{c}{6} \ln \left[\frac{4f(a)f(b)f(q)}{\kappa_h^6 \varepsilon^6} \cosh^2 \kappa_h t_b \right] + \\ &+ \frac{c}{3} \ln \left[\frac{\cosh \kappa_h(r_*(b) - r_*(a)) - \cosh \kappa_h(t_a - t_b)}{\cosh \kappa_h(r_*(q) - r_*(a)) - \cosh \kappa_h(t_a - t_b)} \right] + \\ &+ \frac{c}{3} \ln \left[\cosh \kappa_h(r_*(q) - r_*(b)) - 1 \right]. \end{aligned} \quad (\text{A13})$$

Due to linear growth, there is no solution to the extremization equation for $t_a \approx t_b$.

For intermediate times

$$\begin{aligned} 1 &\ll \cosh \kappa_h(r_*(b) - r_*(a)) \ll x \ll \\ &\ll \cosh \kappa_h(r_*(q) - r_*(b)) < \cosh \kappa_h(r_*(q) - r_*(a)), \end{aligned} \quad (\text{A14})$$

where $x = \cosh \kappa_h(t_a + t_b)$ or $\cosh 2\kappa_h t_b$, making use of (A9) and $t_a, t_b \gg r_h$ we can simplify the generalized

entropy functional to

$$\begin{aligned} S_{\text{gen}}[I_{\text{MS}}, R_{\text{MS}}] \Big|_{\text{inter. times}} &\simeq \frac{2\pi a^2}{G_N} + \\ &+ \frac{c}{6} \ln \left(\frac{4f(a)f(b)f(q)}{\kappa_h^6 \varepsilon^6} \cosh^2 \kappa_h t_b \right) + \\ &+ \frac{c}{3} \kappa_h(r_*(b) - r_*(a)) - \\ &- \frac{2c}{3} \cosh \kappa_h(t_a - t_b) e^{-\kappa_h(r_*(b) - r_*(a))} - \\ &- \frac{c}{3} e^{-\kappa_h(t_a + t_b) + \kappa_h(r_*(b) - r_*(a))} - \\ &- \frac{c}{6} e^{2\kappa_h t_b - \kappa_h(r_*(q) - r_*(b))} + \\ &+ \frac{c}{3} \cosh \kappa_h(t_a - t_b) e^{-\kappa_h(r_*(q) - r_*(a))} + \\ &+ \frac{c}{6} e^{\kappa_h(t_a + t_b) - \kappa_h(r_*(q) - r_*(a))}. \end{aligned} \quad (\text{A15})$$

The extremal curve with respect to time coordinate is at $t_a = t_b$. Using this, we get

$$\begin{aligned} S_{\text{gen}}[I_{\text{MS}}, R_{\text{MS}}] \Big|_{\text{inter. times}} &\simeq \frac{2\pi a^2}{G_N} + \\ &+ \frac{c}{6} \ln \left(\frac{4f(a)f(b)f(q)}{\kappa_h^6 \varepsilon^6} \cosh^2 \kappa_h t_b \right) + \\ &+ \frac{c}{3} \kappa_h(r_*(b) - r_*(a)) - \frac{c}{3} e^{2\kappa_h t_b - \kappa_h(r_*(q) - r_*(b))}. \end{aligned} \quad (\text{A16})$$

We keep the vanishingly small last term from other exponential terms as that describing the leading order effect of the finite size of the region.

Taking then near-horizon-zone ansatz for the radial coordinate of the island, $a = r_h + \delta a$, $\delta a \ll r_h$, we find the analytical expression (35) for the entropy in the leading order in $\delta a/r_h$ without solving extremization equation on a explicitly,

$$\begin{aligned} S_{\text{gen}}^{\text{ext}}[I_{\text{MS}}, R_{\text{MS}}] \Big|_{\text{inter. times}} &\simeq \\ &\simeq \frac{2\pi r_h^2}{G_N} + \frac{c}{6} \ln \frac{f(b)}{\kappa_h^4 \varepsilon^4} + \frac{c}{3} \kappa_h r_*(b) - \frac{c}{6} + \\ &+ \frac{c}{6} \ln \left(\frac{4f(q) \cosh^2 \kappa_h t_b}{\kappa_h^2 \varepsilon^2} \right) - \frac{c}{3} e^{2\kappa_h t_b - \kappa_h(r_*(q) - r_*(b))} + \\ &+ O(\delta a/r_h). \end{aligned} \quad (\text{A17})$$

3. AS entangling region without island

The entanglement entropy for the asymmetric finite entangling region takes the form

$$\begin{aligned}
S(R_{AS}) &= \frac{c}{3} \ln \left(\frac{d(\mathbf{b}_+^{\text{up}}, \mathbf{b}_-^{\text{up}}) d(\mathbf{q}_-^{\text{down}}, \mathbf{b}_-^{\text{up}})}{\varepsilon^2} \right) + \\
&+ \frac{c}{3} \ln \left(\frac{d(\mathbf{b}_+^{\text{up}}, \mathbf{q}_+^{\text{up}}) d(\mathbf{q}_-^{\text{down}}, \mathbf{q}_+^{\text{up}})}{\varepsilon^2} \right) - \\
&- \frac{c}{3} \ln \left(\frac{d(\mathbf{b}_-^{\text{up}}, \mathbf{q}_+^{\text{up}}) d(\mathbf{q}_-^{\text{down}}, \mathbf{b}_+^{\text{up}})}{\varepsilon^2} \right) = \\
&= \frac{c}{6} \ln \left[\frac{16f(b)f(q)}{\kappa_h^4 \varepsilon^4} \cosh^2 \kappa_h t_b \right] + \\
&+ \frac{c}{6} \ln \left[\frac{\cosh \kappa_h(r_*(q) - r_*(b)) - \cosh 2\kappa_h t_b}{\cosh \kappa_h(r_*(q) - r_*(b)) + \cosh 2\kappa_h t_b} \right] + \\
&+ \frac{c}{6} \ln \left[\frac{\cosh \kappa_h(r_*(q) - r_*(b)) - 1}{\cosh \kappa_h(r_*(q) - r_*(b)) + 1} \right]. \tag{A18}
\end{aligned}$$

In the limit $q \rightarrow \infty$, we obtain

$$\lim_{q \rightarrow \infty} S(R_{AS}) = \frac{c}{6} \ln \left(\frac{16f(b)}{\kappa_h^4 \varepsilon^4} \cosh^2 \kappa_h t_b \right). \tag{A19}$$

4. AS entangling region with island

The generalized entropy functional for a general non-symmetric island ansatz is

$$\begin{aligned}
S_{\text{gen}}[I, R_{AS}] &= \frac{\pi(a^2 + p^2)}{G_N} + \\
&+ \frac{c}{6} \ln \left[\frac{32\sqrt{f(a)f(p)f(b)f(q)}}{\kappa_h^6 \varepsilon^6} \cosh^2 \kappa_h t_b \right] + \\
&+ \frac{c}{6} \ln [\cosh \kappa_h(r_*(a) - r_*(p)) + \cosh \kappa_h(t_a + t_p)] + \\
&+ \frac{c}{6} \ln \left[\frac{\cosh \kappa_h(r_*(b) - r_*(a)) - \cosh \kappa_h(t_a - t_b)}{\cosh \kappa_h(r_*(b) - r_*(a)) + \cosh \kappa_h(t_a + t_b)} \right] + \\
&+ \frac{c}{6} \ln \left[\frac{\cosh \kappa_h(r_*(b) - r_*(p)) - \cosh \kappa_h(t_p - t_b)}{\cosh \kappa_h(r_*(b) - r_*(p)) + \cosh \kappa_h(t_p + t_b)} \right] + \\
&+ \frac{c}{6} \ln \left[\frac{\cosh \kappa_h(r_*(q) - r_*(b)) - 1}{\cosh \kappa_h(r_*(q) - r_*(b)) + 1} \right] + \\
&+ \frac{c}{6} \ln \left[\frac{\cosh \kappa_h(r_*(q) - r_*(b)) - \cosh 2\kappa_h t_b}{\cosh \kappa_h(r_*(q) - r_*(b)) + \cosh 2\kappa_h t_b} \right] + \\
&+ \frac{c}{6} \ln \left[\frac{\cosh \kappa_h(r_*(q) - r_*(a)) + \cosh \kappa_h(t_a - t_b)}{\cosh \kappa_h(r_*(q) - r_*(a)) - \cosh \kappa_h(t_a - t_b)} \right] + \\
&+ \frac{c}{6} \ln \left[\frac{\cosh \kappa_h(r_*(q) - r_*(p)) + \cosh \kappa_h(t_p + t_b)}{\cosh \kappa_h(r_*(q) - r_*(p)) - \cosh \kappa_h(t_p + t_b)} \right]. \tag{A20}
\end{aligned}$$

The only non-symmetric under exchange $a \leftrightarrow p$, $t_a \leftrightarrow t_p$ terms in this expression are in the last two lines. These terms are vanishingly small for times such that

$$\begin{aligned}
\cosh \kappa_h(t_p + t_b) &\ll \cosh \kappa_h(r_*(q) - r_*(p)), \\
\cosh \kappa_h(t_a - t_b) &\ll \cosh \kappa_h(r_*(q) - r_*(a)). \tag{A21}
\end{aligned}$$

Under these assumptions taking the mirror-symmetric ansatz for island $I_{\text{MS}} = [\mathbf{a}_-, \mathbf{a}_+]$ is valid. Substituting it to $S[I, R_{AS}]$, we arrive at

$$\begin{aligned}
S_{\text{gen}}[I_{\text{MS}}, R_{AS}] &\simeq \frac{2\pi a^2}{G_N} + \\
&+ \frac{c}{6} \ln \left[\frac{64f(a)f(b)f(q)}{\kappa_h^6 \varepsilon^6} \cosh^2 \kappa_h t_a \cosh^2 \kappa_h t_b \right] + \\
&+ \frac{c}{3} \ln \left[\frac{\cosh \kappa_h(r_*(b) - r_*(a)) - \cosh \kappa_h(t_a - t_b)}{\cosh \kappa_h(r_*(b) - r_*(a)) + \cosh \kappa_h(t_a + t_b)} \right] + \\
&+ \frac{c}{6} \ln \left[\frac{\cosh \kappa_h(r_*(q) - r_*(b)) - 1}{\cosh \kappa_h(r_*(q) - r_*(b)) + 1} \right] + \\
&+ \frac{c}{6} \ln \left[\frac{\cosh \kappa_h(r_*(q) - r_*(b)) - \cosh 2\kappa_h t_b}{\cosh \kappa_h(r_*(q) - r_*(b)) + \cosh 2\kappa_h t_b} \right] + \\
&+ \frac{c}{6} \ln \left[\frac{\cosh \kappa_h(r_*(q) - r_*(a)) + \cosh \kappa_h(t_a - t_b)}{\cosh \kappa_h(r_*(q) - r_*(a)) - \cosh \kappa_h(t_a - t_b)} \right] + \\
&+ \frac{c}{6} \ln \left[\frac{\cosh \kappa_h(r_*(q) - r_*(a)) + \cosh \kappa_h(t_a + t_b)}{\cosh \kappa_h(r_*(q) - r_*(a)) - \cosh \kappa_h(t_a + t_b)} \right]. \tag{A22}
\end{aligned}$$

If we then assume that the island endpoints are near the horizon and times are long before the Cauchy surface breaking (36) (intermediate times), such that

$$\begin{aligned}
1 &\ll \cosh \kappa_h(r_*(b) - r_*(a)) \ll x \ll \\
&\ll \cosh \kappa_h(r_*(q) - r_*(b)) < \cosh \kappa_h(r_*(q) - r_*(a)), \tag{A23}
\end{aligned}$$

where $x = \cosh \kappa_h(t_a + t_b)$ or $\cosh 2\kappa_h t_b$, making use of (A9) and $t_a, t_b \gg r_h$ we can simplify the generalized entropy functional to

$$\begin{aligned}
S_{\text{gen}}[I_{\text{MS}}, R_{AS}] \Big|_{\text{inter. times}} &\simeq \frac{2\pi a^2}{G_N} + \\
&+ \frac{c}{6} \ln \left(\frac{4f(a)f(b)f(q)}{\kappa_h^6 \varepsilon^6} \right) + \frac{c}{3} \kappa_h(r_*(b) - r_*(a)) - \\
&- \frac{2c}{3} \cosh \kappa_h(t_a - t_b) e^{-\kappa_h(r_*(b) - r_*(a))} - \\
&- \frac{c}{3} e^{-\kappa_h(t_a + t_b) + \kappa_h(r_*(b) - r_*(a))} - \\
&- \frac{c}{3} e^{2\kappa_h t_b - \kappa_h(r_*(q) - r_*(b))} + \\
&+ \frac{2c}{3} \cosh \kappa_h(t_a - t_b) e^{-\kappa_h(r_*(q) - r_*(a))} + \\
&+ \frac{c}{3} e^{\kappa_h(t_a + t_b) - \kappa_h(r_*(q) - r_*(a))}. \tag{A24}
\end{aligned}$$

Extremizing with respect to t_a , we obtain

$$\begin{aligned}
S_{\text{gen}}[I_{\text{MS}}, R_{AS}] \Big|_{\text{inter. times}} &\simeq \frac{2\pi a^2}{G_N} + \frac{c}{6} \ln \left(\frac{4f(a)f(b)f(q)}{\kappa_h^6 \varepsilon^6} \right) + \\
&+ \frac{c}{3} \kappa_h(r_*(b) - r_*(a)) - \frac{c}{3} e^{2\kappa_h t_b - \kappa_h(r_*(q) - r_*(b))}, \tag{A25}
\end{aligned}$$

and hence an approximate analytical expression (39) in

the near-horizon zone in the leading order in $\delta a/r_h$ is

$$\begin{aligned}
S_{\text{gen}}^{\text{ext}}[I_{\text{MS}}, R_{\text{AS}}] \Big|_{\text{inter. times}} &\simeq \\
&\simeq \frac{2\pi r_h^2}{G_N} + \frac{c}{6} \ln \frac{f(b)}{\kappa_h^4 \varepsilon^4} + \frac{c}{3} \kappa_h r_*(b) - \frac{c}{6} + \\
&+ \frac{c}{6} \ln \frac{4f(q)}{\kappa_h^2 \varepsilon^2} - \frac{c}{3} e^{2\kappa_h t_b - \kappa_h(r_*(q) - r_*(b))} + O(\delta a/r_h).
\end{aligned} \tag{A26}$$

5. Outer entangling region for AS finite region

The entanglement entropy for C_{AS} takes the form

$$\begin{aligned}
S_m(C_{\text{AS}}) &= \lim_{w \rightarrow \infty} \left[\frac{c}{3} \ln \left(\frac{d(\mathbf{q}_+^{\text{up}}, \mathbf{q}_-^{\text{down}}) d(\mathbf{q}_+^{\text{up}}, \mathbf{w}_+^{\text{up}})}{\varepsilon^2} \right) + \right. \\
&+ \frac{c}{3} \ln \left(\frac{d(\mathbf{w}_-^{\text{down}}, \mathbf{q}_-^{\text{down}}) d(\mathbf{w}_-^{\text{down}}, \mathbf{w}_+^{\text{up}})}{\varepsilon^2} \right) - \\
&- \left. \frac{c}{3} \ln \left(\frac{d(\mathbf{w}_-^{\text{down}}, \mathbf{q}_+^{\text{up}}) d(\mathbf{w}_+^{\text{up}}, \mathbf{q}_-^{\text{down}})}{\varepsilon^2} \right) \right] = \\
&= \lim_{w \rightarrow \infty} \frac{c}{6} \ln \left(\frac{16f(q)f(w)}{\kappa_h^4 \varepsilon^4} \right) + \\
&+ \lim_{w \rightarrow \infty} \frac{c}{3} \ln \left(\frac{\cosh \kappa_h(r_*(w) - r_*(q)) - 1}{\cosh \kappa_h(r_*(w) - r_*(q)) + 1} \right) = \\
&= \frac{c}{6} \ln \frac{4f(q)}{\kappa_h^2 \varepsilon^2} + \frac{c}{3} \ln \frac{2}{\kappa_h \varepsilon}.
\end{aligned} \tag{A27}$$

According to our prescription for IR regularization, the latter term is to be subtracted. Interestingly, the same result can be obtained if C_{AS} is considered as the complement of the regularized Cauchy surface. The entropy for it we have already calculated in (19), $S_m(C_{\text{AS}}) = S_m(\bar{\Sigma}_{\text{reg}})$.

-
- [1] S. W. Hawking, Particle creation by black holes, *Comm. Math. Phys.* **43**, 199 (1975).
 - [2] S. W. Hawking, Breakdown of Predictability in Gravitational Collapse, *Phys. Rev. D* **14**, 2460 (1976).
 - [3] D. N. Page, Information in black hole radiation, *Phys. Rev. Lett.* **71**, 3743 (1993), arXiv:hep-th/9306083.
 - [4] D. N. Page, Time Dependence of Hawking Radiation Entropy, *JCAP* **09**, 028, arXiv:1301.4995 [hep-th].
 - [5] G. Penington, Entanglement Wedge Reconstruction and the Information Paradox, *JHEP* **09**, 002, arXiv:1905.08255 [hep-th].
 - [6] A. Almheiri, N. Engelhardt, D. Marolf, and H. Maxfield, The entropy of bulk quantum fields and the entanglement wedge of an evaporating black hole, *JHEP* **12**, 063, arXiv:1905.08762 [hep-th].
 - [7] A. Almheiri, R. Mahajan, J. Maldacena, and Y. Zhao, The Page curve of Hawking radiation from semiclassical geometry, *JHEP* **03**, 149, arXiv:1908.10996 [hep-th].
 - [8] P. C. W. Davies and S. A. Fulling, Radiation from a moving mirror in two-dimensional space-time conformal anomaly, *Proc. Roy. Soc. Lond. A* **348**, 393 (1976).
 - [9] M. R. R. Good, K. Yelshibekov, and Y. C. Ong, On Horizonless Temperature with an Accelerating Mirror, *JHEP* **03**, 013, arXiv:1611.00809 [gr-qc].
 - [10] P. Chen and D.-h. Yeom, Entropy evolution of moving mirrors and the information loss problem, *Phys. Rev. D* **96**, 025016 (2017), arXiv:1704.08613 [hep-th].
 - [11] M. R. R. Good, E. V. Linder, and F. Wilczek, Moving mirror model for quasithermal radiation fields, *Phys. Rev. D* **101**, 025012 (2020), arXiv:1909.01129 [gr-qc].
 - [12] A. Almheiri, R. Mahajan, and J. Maldacena, Islands outside the horizon, (2019), arXiv:1910.11077 [hep-th].
 - [13] M. Rozali, J. Sully, M. Van Raamsdonk, C. Waddell, and D. Wakeham, Information radiation in BCFT models of black holes, *JHEP* **05**, 004, arXiv:1910.12836 [hep-th].
 - [14] G. Penington, S. H. Shenker, D. Stanford, and Z. Yang, Replica wormholes and the black hole interior, *JHEP* **03**, 205, arXiv:1911.11977 [hep-th].
 - [15] A. Almheiri, T. Hartman, J. Maldacena, E. Shaghoulian, and A. Tajdini, Replica Wormholes and the Entropy of Hawking Radiation, *JHEP* **05**, 013, arXiv:1911.12333 [hep-th].
 - [16] F. F. Gautason, L. Schneiderbauer, W. Sybesma, and L. Thorlacius, Page Curve for an Evaporating Black Hole, *JHEP* **05**, 091, arXiv:2004.00598 [hep-th].
 - [17] T. Anegawa and N. Iizuka, Notes on islands in asymptotically flat 2d dilaton black holes, *JHEP* **07**, 036, arXiv:2004.01601 [hep-th].

- [18] K. Hashimoto, N. Iizuka, and Y. Matsuo, Islands in Schwarzschild black holes, JHEP **06**, 085, arXiv:2004.05863 [hep-th].
- [19] J. Sully, M. Van Raamsdonk, and D. Wakeham, BCFT entanglement entropy at large central charge and the black hole interior, JHEP **03**, 167, arXiv:2004.13088 [hep-th].
- [20] T. Hartman, E. Shaghoulian, and A. Strominger, Islands in Asymptotically Flat 2D Gravity, JHEP **07**, 022, arXiv:2004.13857 [hep-th].
- [21] C. Krishnan, V. Patil, and J. Pereira, Page Curve and the Information Paradox in Flat Space, (2020), arXiv:2005.02993 [hep-th].
- [22] M. Alishahiha, A. Faraji Astaneh, and A. Naseh, Island in the presence of higher derivative terms, JHEP **02**, 035, arXiv:2005.08715 [hep-th].
- [23] H. Geng and A. Karch, Massive islands, JHEP **09**, 121, arXiv:2006.02438 [hep-th].
- [24] H. Z. Chen, R. C. Myers, D. Neuenfeld, I. A. Reyes, and J. Sandor, Quantum Extremal Islands Made Easy, Part I: Entanglement on the Brane, JHEP **10**, 166, arXiv:2006.04851 [hep-th].
- [25] A. Almheiri, T. Hartman, J. Maldacena, E. Shaghoulian, and A. Tajdini, The entropy of Hawking radiation, Rev. Mod. Phys. **93**, 035002 (2021), arXiv:2006.06872 [hep-th].
- [26] X. Dong, X.-L. Qi, Z. Shangnan, and Z. Yang, Effective entropy of quantum fields coupled with gravity, JHEP **10**, 052, arXiv:2007.02987 [hep-th].
- [27] V. Balasubramanian, A. Kar, and T. Ugajin, Islands in de Sitter space, JHEP **02**, 072, arXiv:2008.05275 [hep-th].
- [28] W. Sybesma, Pure de Sitter space and the island moving back in time, Class. Quant. Grav. **38**, 145012 (2021), arXiv:2008.07994 [hep-th].
- [29] H. Z. Chen, R. C. Myers, D. Neuenfeld, I. A. Reyes, and J. Sandor, Quantum Extremal Islands Made Easy, Part II: Black Holes on the Brane, JHEP **12**, 025, arXiv:2010.00018 [hep-th].
- [30] Y. Ling, Y. Liu, and Z.-Y. Xian, Island in Charged Black Holes, JHEP **03**, 251, arXiv:2010.00037 [hep-th].
- [31] Y. Matsuo, Islands and stretched horizon, JHEP **07**, 051, arXiv:2011.08814 [hep-th].
- [32] K. Goto, T. Hartman, and A. Tajdini, Replica wormholes for an evaporating 2D black hole, JHEP **04**, 289, arXiv:2011.09043 [hep-th].
- [33] I. Aka, Y. Kusuki, N. Shiba, T. Takayanagi, and Z. Wei, Entanglement Entropy in a Holographic Moving Mirror and the Page Curve, Phys. Rev. Lett. **126**, 061604 (2021), arXiv:2011.12005 [hep-th].
- [34] H. Geng, A. Karch, C. Perez-Pardavila, S. Raju, L. Randall, M. Riojas, and S. Shashi, Information Transfer with a Gravitating Bath, SciPost Phys. **10**, 103 (2021), arXiv:2012.04671 [hep-th].
- [35] G. K. Karananas, A. Kehagias, and J. Taskas, Islands in linear dilaton black holes, JHEP **03**, 253, arXiv:2101.00024 [hep-th].
- [36] X. Wang, R. Li, and J. Wang, Islands and Page curves of Reissner-Nordström black holes, JHEP **04**, 103, arXiv:2101.06867 [hep-th].
- [37] K. Kawabata, T. Nishioka, Y. Okuyama, and K. Watanabe, Probing Hawking radiation through capacity of entanglement, JHEP **05**, 062, arXiv:2102.02425 [hep-th].
- [38] I. A. Reyes, Moving Mirrors, Page Curves, and Bulk Entropies in AdS2, Phys. Rev. Lett. **127**, 051602 (2021), arXiv:2103.01230 [hep-th].
- [39] H. Geng, Y. Nomura, and H.-Y. Sun, Information paradox and its resolution in de Sitter holography, Phys. Rev. D **103**, 126004 (2021), arXiv:2103.07477 [hep-th].
- [40] A. Bhattacharya, A. Bhattacharyya, P. Nandy, and A. K. Patra, Islands and complexity of eternal black hole and radiation subsystems for a doubly holographic model, JHEP **05**, 135, arXiv:2103.15852 [hep-th].
- [41] W. Kim and M. Nam, Entanglement entropy of asymptotically flat non-extremal and extremal black holes with an island, Eur. Phys. J. C **81**, 869 (2021), arXiv:2103.16163 [hep-th].
- [42] L. Aalsma and W. Sybesma, The Price of Curiosity: Information Recovery in de Sitter Space, JHEP **05**, 291, arXiv:2104.00006 [hep-th].
- [43] H. Geng, S. Lüster, R. K. Mishra, and D. Wakeham, Holographic BCFTs and Communicating Black Holes, JHEP **08**, 003 (2021), arXiv:2104.07039 [hep-th].
- [44] Y. Lu and J. Lin, Islands in Kaluza-Klein black holes, Eur. Phys. J. C **82**, 132 (2022), arXiv:2106.07845 [hep-th].
- [45] I. Aka, Y. Kusuki, N. Shiba, T. Takayanagi, and Z. Wei, Holographic moving mirrors, Class. Quant. Grav. **38**, 224001 (2021), arXiv:2106.11179 [hep-th].
- [46] M.-H. Yu and X.-H. Ge, Islands and Page curves in charged dilaton black holes, Eur. Phys. J. C **82**, 14 (2022), arXiv:2107.03031 [hep-th].
- [47] H. Geng, A. Karch, C. Perez-Pardavila, S. Raju, L. Randall, M. Riojas, and S. Shashi, Inconsistency of islands in theories with long-range gravity, JHEP **01**, 182, arXiv:2107.03390 [hep-th].
- [48] B. Ahn, S.-E. Bak, H.-S. Jeong, K.-Y. Kim, and Y.-W. Sun, Islands in charged linear dilaton black holes, Phys. Rev. D **105**, 046012 (2022), arXiv:2107.07444 [hep-th].
- [49] D. S. Ageev, Shaping contours of entanglement islands in BCFT, JHEP **03**, 033, arXiv:2107.09083 [hep-th].
- [50] V. Balasubramanian, B. Craps, M. Khramtsov, and E. Shaghoulian, Submerging islands through thermalization, JHEP **10**, 048, arXiv:2107.14746 [hep-th].
- [51] N. H. Cao, Entanglement entropy and Page curve of black holes with island in massive gravity, Eur. Phys. J. C **82**, 381 (2022), arXiv:2108.10144 [hep-th].
- [52] D. Fernández-Silvestre, J. Foo, and M. R. R. Good, On the duality of Schwarzschild-de Sitter spacetime and moving mirror, Class. Quant. Grav. **39**, 055006 (2022), arXiv:2109.04147 [gr-qc].
- [53] S. Azarnia, R. Fareghbal, A. Naseh, and H. Zolfi, Islands in flat-space cosmology, Phys. Rev. D **104**, 126017 (2021), arXiv:2109.04795 [hep-th].
- [54] A. Bhattacharya, A. Bhattacharyya, P. Nandy, and A. K. Patra, Partial islands and subregion complexity in geometric secret-sharing model, JHEP **12**, 091, arXiv:2109.07842 [hep-th].
- [55] I. Aref'eva and I. Volovich, A Note on Islands in Schwarzschild Black Holes, (2021), arXiv:2110.04233 [hep-th].
- [56] S. He, Y. Sun, L. Zhao, and Y.-X. Zhang, The universality of islands outside the horizon, JHEP **05**, 047, arXiv:2110.07598 [hep-th].
- [57] D. S. Ageev, I. Y. Aref'eva, and A. V. Lysukhina, Wormholes in Jackiw-Teitelboim Gravity, Teor. Mat. Fiz. **201**, 424 (2019).

- [58] F. Omid, Entropy of Hawking radiation for two-sided hyperscaling violating black branes, *JHEP* **04**, 022, arXiv:2112.05890 [hep-th].
- [59] A. Bhattacharya, A. Bhattacharyya, P. Nandy, and A. K. Patra, Bath deformations, islands, and holographic complexity, *Phys. Rev. D* **105**, 066019 (2022), arXiv:2112.06967 [hep-th].
- [60] H. Geng, A. Karch, C. Perez-Pardavila, S. Raju, L. Randall, M. Riojas, and S. Shashi, Entanglement phase structure of a holographic BCFT in a black hole background, *JHEP* **05**, 153, arXiv:2112.09132 [hep-th].
- [61] M.-H. Yu, C.-Y. Lu, X.-H. Ge, and S.-J. Sin, Island, Page curve, and superradiance of rotating BTZ black holes, *Phys. Rev. D* **105**, 066009 (2022), arXiv:2112.14361 [hep-th].
- [62] K. Suzuki and T. Takayanagi, BCFT and Islands in two dimensions, *JHEP* **06**, 095, arXiv:2202.08462 [hep-th].
- [63] Q.-L. Hu, D. Li, R.-X. Miao, and Y.-Q. Zeng, AdS/BCFT and Island for curvature-squared gravity, *JHEP* **09**, 037, arXiv:2202.03304 [hep-th].
- [64] P.-J. Hu, D. Li, and R.-X. Miao, Island on codimension-two branes in AdS/dCFT, *JHEP* **11**, 008, arXiv:2208.11982 [hep-th].
- [65] I. Y. Aref'eva, T. A. Rusalev, and I. V. Volovich, Entanglement entropy of a near-extremal black hole, *Teor. Mat. Fiz.* **212**, 457 (2022), arXiv:2202.10259 [hep-th].
- [66] W.-C. Gan, D.-H. Du, and F.-W. Shu, Island and Page curve for one-sided asymptotically flat black hole, *JHEP* **07**, 020, arXiv:2203.06310 [hep-th].
- [67] J. Basak Kumar, D. Basu, V. Malvimat, H. Parihar, and G. Sengupta, Reflected entropy and entanglement negativity for holographic moving mirrors, *JHEP* **09**, 089, arXiv:2204.06015 [hep-th].
- [68] S. Azarnia and R. Fareghbal, Islands in Kerr-de Sitter spacetime and their flat limit, *Phys. Rev. D* **106**, 026012 (2022), arXiv:2204.08488 [hep-th].
- [69] I. Akal, T. Kawamoto, S.-M. Ruan, T. Takayanagi, and Z. Wei, Zoo of holographic moving mirrors, *JHEP* **08**, 296, arXiv:2205.02663 [hep-th].
- [70] M. Afrasiar, J. Kumar Basak, A. Chandra, and G. Sengupta, Islands for Entanglement Negativity in Communicating Black Holes, (2022), arXiv:2205.07903 [hep-th].
- [71] A. Anand, Page Curve and Island in EGB gravity, (2022), arXiv:2205.13785 [hep-th].
- [72] D. S. Ageev and I. Y. Aref'eva, Thermal density matrix breaks down the Page curve, *Eur. Phys. J. Plus* **137**, 1188 (2022), arXiv:2206.04094 [hep-th].
- [73] S. Djordjević, A. Gočanin, D. Gočanin, and V. Radovanović, Page curve for an eternal Schwarzschild black hole in a dimensionally reduced model of dilaton gravity, *Phys. Rev. D* **106**, 105015 (2022), arXiv:2207.07409 [hep-th].
- [74] K. Goswami and K. Narayan, Small Schwarzschild de Sitter black holes, quantum extremal surfaces and islands, *JHEP* **10**, 031, arXiv:2207.10724 [hep-th].
- [75] A. Roy Chowdhury, A. Saha, and S. Gangopadhyay, Role of mutual information in the Page curve, *Phys. Rev. D* **106**, 086019 (2022), arXiv:2207.13029 [hep-th].
- [76] H. Geng, L. Randall, and E. Swanson, BCFT in a Black Hole Background: An Analytical Holographic Model, (2022), arXiv:2209.02074 [hep-th].
- [77] S. N. Solodukhin, Entanglement entropy of black holes, *Living Rev. Rel.* **14**, 8 (2011), arXiv:1104.3712 [hep-th].
- [78] T. Nishioka, Entanglement entropy: holography and renormalization group, *Rev. Mod. Phys.* **90**, 035007 (2018), arXiv:1801.10352 [hep-th].
- [79] H. Casini, C. D. Fosco, and M. Huerta, Entanglement and alpha entropies for a massive Dirac field in two dimensions, *J. Stat. Mech.* **0507**, P07007 (2005), arXiv:cond-mat/0505563.
- [80] J. Cotler, P. Hayden, G. Penington, G. Salton, B. Swingle, and M. Walter, Entanglement Wedge Reconstruction via Universal Recovery Channels, *Phys. Rev. X* **9**, 031011 (2019), arXiv:1704.05839 [hep-th].
- [81] J. B. Hartle and S. W. Hawking, Wave Function of the Universe, *Phys. Rev. D* **28**, 2960 (1983).
- [82] P. Calabrese and J. L. Cardy, Entanglement entropy and quantum field theory, *J. Stat. Mech.* **0406**, P06002 (2004), arXiv:hep-th/0405152.
- [83] P. Calabrese and J. Cardy, Entanglement entropy and conformal field theory, *J. Phys. A* **42**, 504005 (2009), arXiv:0905.4013 [cond-mat.stat-mech].
- [84] T. Hartman and J. Maldacena, Time Evolution of Entanglement Entropy from Black Hole Interiors, *JHEP* **05**, 014, arXiv:1303.1080 [hep-th].